ACADÉMIE
DES SCIENCES
INSTITUT DE FRANCE

Comptes Rendus

Géoscience

Sciences de la Planète

Jacques Dili-Rake, Daouda Dawaï, Benoît Joseph Mbassa,
Olivier Vanderhaeghe, Michel Grégoire, Mathieu Benoit and Rachid Zayane

Origin and petrogenesis of volcanic rocks from Ziver in Northern Cameroon (Cameroon–Chad Volcanic Line, Central Africa): insights from mineralogical, geochemical and isotopic data

Volume 358 (2026), p. 331-352

Online since: 1 June 2026

https://doi.org/10.5802/crgeos.336

The Comptes Rendus. Géoscience — Sciences de la Planète *are a member of the Mersenne Center for open scientific publishing*
www.centre-mersenne.org — e-ISSN : 1778-7025

ACADÉMIE DES SCIENCES
INSTITUT DE FRANCE

Comptes Rendus. Géoscience — Sciences de la Planète
2026, Vol. 358, p. 331-352
https://doi.org/10.5802/crgeos.336

Research article
Petrology, petrophysics

Origin and petrogenesis of volcanic rocks from Ziver in Northern Cameroon (Cameroon–Chad Volcanic Line, Central Africa): insights from mineralogical, geochemical and isotopic data

Jacques Dili-Rake [a,b], Daouda Dawaï [b], Benoît Joseph Mbassa [*,a], Olivier Vanderhaeghe [c], Michel Grégoire [c], Mathieu Benoit [c] and Rachid Zayane [d]

[a] Institute of Geological and Mining Research, PO Box 4110, Yaoundé, Cameroon

[b] Department of Earth Sciences, Faculty of Sciences, University of Maroua, PO Box 814 Maroua, Cameroon

[c] GET-OMP, Université de Toulouse, UPS, CNRS, IRD, CNES, 14 avenue E. Belin, 31400 Toulouse, France

[d] Geology Department, Cadi Ayyad University, BP 2390, 40000 Marrakech, Morocco

E-mail: benjo_mbassa@yahoo.fr (B. J. Mbassa)

Abstract. The Ziver volcanism, located in northern Cameroon within the Central African Rift, forms an integral part of the Cameroon–Chad Volcanic Line (CCVL). The new mineralogical, geochemical, and isotopic data presented here provide fresh insights into the sources and petrogenesis of lavas from this little-studied area. The primary mineral assemblage consists of olivine, clinopyroxene, Fe–Ti oxides, and feldspars. Clinopyroxenes are predominantly calcic, with compositions ranging from diopside to clinoenstatite. Feldspars occur as andesine in mafic rocks, whereas in felsic lavas they are represented by K-albite and Na-sanidine. The volcanic suite defines a bimodal alkaline series composed of mafic (basanite, basalt, hawaiite) and felsic (trachyte, rhyolite) lavas, characterized by moderate to high alkali contents ($K_2O + Na_2O$ = 4.10–12.25 wt%). These lavas display moderately enriched radiogenic isotope signatures, with $^{87}Sr/^{86}Sr$ ratios of 0.70311–0.71856 and $^{143}Nd/^{144}Nd$ ratios of 0.51276–0.51295. Geochemical and isotopic data ($0.7036 < (^{87}Sr/^{86}Sr)_{initial} < 0.7203$; $-10.65 < \varepsilon Ndi < 6.44$) indicate an intraplate OIB affinity, derived from low-degree (1–3%) partial melting of an enriched garnet lherzolite mantle plume source. Magmatic differentiation is dominated by fractional crystallization with minimal crustal contamination, consistent with the CCVL as a whole.

Keywords. Cameroon–Chad Volcanic Line, Ziver volcanic rocks, Bimodal alkaline suite, Mantle origin, Fractional crystallization.

Funding. CNRS–IRD–LithoCOAC project.

Manuscript received 6 December 2025, revised 9 March 2026, accepted 7 April 2026, online since 1 June 2026.

1. Introduction

Alkaline magmatism is a key indicator of various tectonic settings, including oceanic hotspots and seamounts (Kogarko, 1998; Hart et al., 1992), continental rifts, and other intraplate environments (Corfu et al., 1991). Its genesis occurs at different depths within the mantle, ranging from the asthenosphere to the core-mantle boundary. This type of

*Corresponding author

magmatism significantly contributes to continental crust evolution and reflects intricate interactions between Earth's geospheres. The generation of alkaline magmas is commonly attributed to several mantle processes. One widely invoked mechanism is the low-degree partial melting of peridotites in the presence of CO_2, which lowers the solidus and favors the production of silica-undersaturated melts. Alternatively, alkaline magmas may derived from the melting of recycled oceanic crust as proposed by Hofmann et al. (1986), where subducted basaltic-gabbroic lithologies are returned to the mantle and later re-melted. A third possibility involves the melting of metasomatized lithospheric mantle enriched by fluids or melts from earlier subduction or plume-related events, producing alkaline signatures even at relatively shallow depths (Dasgupta et al., 2007).

The Cameroon–Chad Volcanic Line (CCVL) is a prominent intraplate volcano-tectonic megastructure located in the heart of Central Africa. The lavas along the CCVL are predominantly alkaline (Marzoli, Piccirillo, et al., 2000; Kamgang, Chazot, et al., 2013; Pouclet et al., 2014) despite the occurrences of a few transitional lavas in the West Cameroon Highlands (Fosso et al., 2005; Kuepouo et al., 2006; Ziem à Bidias et al., 2018; Lemdjou et al., 2020), and rare of tholeiitic rocks in Kapsiki (Ngounouno, Déruelle, Guiraud, et al., 2001). In general, the evolution of felsic lavas is driven by the fractional crystallization of mafic rocks coupled with crustal contamination (Kamgang, Chazot, et al., 2013; Tchuimegnie Ngongang et al., 2015).

The northern portion of the CCVL, which includes our study area, remains relatively under-investigated (Figure 1b). However, some geochemical studies have been conducted in some neighboring localities such as the Kapsiki Mountains (Ngounouno and Déruelle, 1997; Tamen et al., 2015), Mandara Mountains (Ngounouno and Déruelle, 1997), Biu Plateau (Rankenburg et al., 2005), Gawar and Zamaï (Gountié Dedzo, Asobo, et al., 2019), Mokolo Hossehone (Tchouhla et al., 2023), and Iriba in the Ouddaï massif Chad (Djerossem et al., 2024).

The volcanic lavas of the Ziver area exhibit a wide range of lithologies, from basanites to rhyolites partially covering the Pan-African granitic basement (Figure 1c). A comprehensive study of these rocks could provide valuable insights into the magmatic source and differentiation processes of this segment of the CCVL. In this study, we present bulk rock major and trace element compositions, along with mineralogical and Sr–Nd isotopic data of the Ziver lavas. Our primary objective is to decipher their magmatic source, discuss their petrogenetic and differentiation processes, and compare them with surrounding lavas to enhance a better understanding of the magmatic evolution in the northern CCVL.

2. Geological setting

The CCVL is structurally localized along the Central Africa Rift System and subdivided into a complex network of faults oriented in three major directions: N30°E, N70°E, and N120°–N130°E (Moreau et al., 1987). This feature is characterized by an N30°E alignment of oceanic and continental volcanic massifs, tracing a path along the Central African Rift (Njome and De Wit, 2014). Extending from Pagalu Island in the Atlantic Ocean, onto the continent (Gountié Dedzo, Asobo, et al., 2019), the CCVL is linked to the reactivation of large intracontinental structures (Cornacchia and Dars, 1983). Some researchers propose its extension to the Tibesti Massif via Lake Chad (Figure 1a) (Déruelle, Bardintzeff, et al., 2000; Djerossem et al., 2024), an extension that has recently led to the alternative designation "Cameroon–Chad Volcanic Line" by Djerossem et al. (2024). Magmatic activity along the CCVL began approximately 67 ± 2 Ma ago (Njonfang, Nono, et al., 2011, and references therein) and continues to the present day, as evidenced by the 1999 and 2000 eruptions of Mount Cameroon (Suh et al., 2003). The origin of magma remains a longstanding debate, and several hypotheses have been proposed, including: (i) Marzoli, Renne, et al. (1999) concluded that the CCVL as a whole cannot be interpreted as the surface expression of simple hotspot magmatism, confirming the earlier conclusions of (Fitton and Dunlop, 1985), drawn from a more restricted database. However, some recent geological data also show that the CCVL lavas do not have the same mantle sources as the St Helena plume, suggesting that the plume is not the source of the CCVL (Marzoli, Piccirillo, et al., 2000; Rankenburg et al., 2005; Yokoyama et al., 2007; Lemdjou et al., 2020); (ii) the development of volcanism has been linked to several hotspots (Ngounouno, Déruelle, Demaiffe and Montigny, 2003; Ngako et al., 2006; Déruelle,

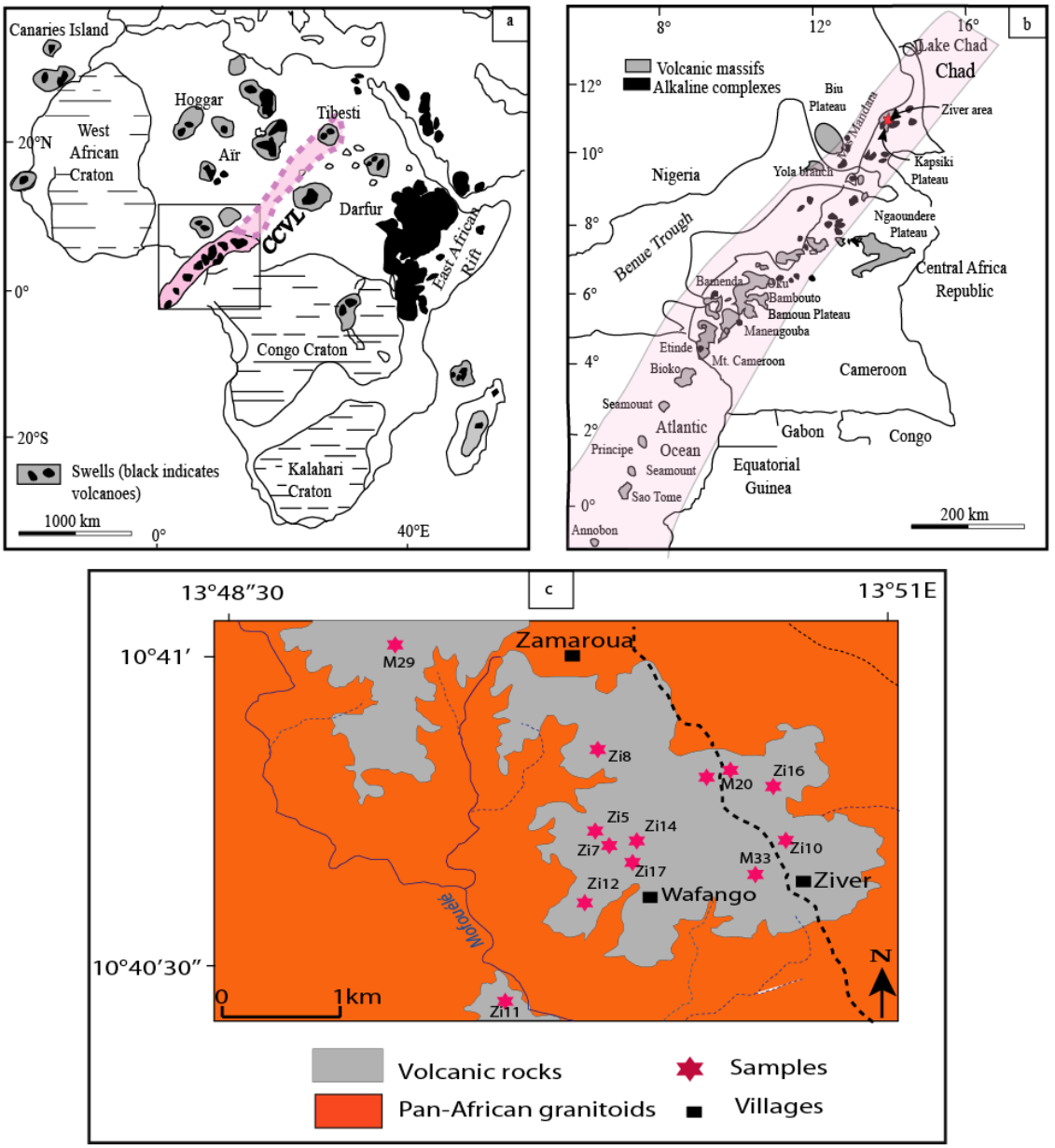

Figure 1. The Cameroon Chad Volcanic Line (CCVL) and its extension. (a) Map illustrating the location of CCVL and its northern extension into Chad, highlighted in pink. The map shows key geological features of the African continent. (b) Detailed map showing the distribution of the major volcanic centers and alkaline complexes along the CCVL. The Chad branch is defined according to Djerossem et al. (2024). The red stars indicates the studied area. (c) Simplified geological sketch map of the Ziver area, showing the locations of collected samples (red stars).

Ngounouno, et al., 2007) or to small-scale tectonics and convection in the upper mantle at the base of the lithosphere (King and Ritsema, 2000; Reusch et al., 2011; De Plean et al., 2014; Adams et al., 2015); (iii) a lateral flow of asthenospheric plumes below the continental lithosphere, which was significantly thinned during Mesozoic rifting, and which could currently contribute to young volcanism along the LVC (Ebinger and Sleep, 1998); (iv) Nkono et al. (2014) and Noudiedie Kamgang et al. (2020) propose two

successive senestrial geodynamic models to explain the distribution of magmatic activity from the Cenozoic to the present. The first, during the Palaeogene, developed around the N70°E direction, while the second (Neogene) is oriented around the N130°E direction. A short transition separates the two periods. The location follows the local reactivation of pre-existing faults (Pan-African) in relation to the collision between the Afro–Arabic and Eurasian plates, during Alpine history.

The lithospheric mantle beneath the CCVL may have undergone both thermochemically and mechanically erosion during the break-up of Gondwana and the opening of the Central Atlantic Ocean (from ~126–100 Ma) (Déruelle, Ngounouno, et al., 2007). Major volcanic activity along the CCVL has been ongoing since cretaceous (68.8 + 1.7 Ma in the Bamoun plateau, (Njonfang, Nono, et al., 2011; Ngonge et al., 2014) and continues to the Present with the eruption of Mount Cameroon (Suh et al., 2003; Déruelle, Ngounouno, et al., 2007). The evolution of silicic lavas through fractional crystallization of mafic terms is overall accompanied by crustal contamination (Kamgang, Chazot, et al., 2013; Tchuimegnie Ngongang et al., 2015). The lavas are mainly basaltic at Mount Cameroon (Déruelle, N'ni, et al., 1987) and remain the dominant composition in the other massifs except in the northern part of the CCVL (Tamen, 1998; Ngounouno, Déruelle and Demaiffe, 2000). Mafic lavas are generally present in all volcanic centers of the CCVL, with the exception of Mount Etindé, which consists of nephelinites, leucitites and haüynophyres (Nkoumbou et al., 1995). The evolved lavas consist of trachyte, trachyphonolite, rhyolite, and phonolite. The compositional gaps observed in most series reflect the strongly bimodal (mafic, and felsic) character of volcanic centres such as Mount Bambouto (Marzoli, Renne, et al., 1999; Youmen et al., 2005; Kagou Dongmo et al., 2010; Gountié Dedzo, Nedelec, et al., 2011), Bamenda Oku (Fitton, 1987), and the Kapsiki plateau (Ngounouno and Déruelle, 1997; Ngounouno, Déruelle and Demaiffe, 2000). The geochemical data reviewed by Déruelle, Moreau, et al. (1991) and Njonfang, Kamgang, et al. (1992) supplemented by numerous detailed studies, show the alkaline nature of the lavas from CCVL, despite the presence of some transitional lavas in the Bamoun Plateau, Mounts Bangou, Bana and Mboutou anorogenic complex.

Geophysical studies (Browne and Fairhead, 1983; Poudjom Djomani et al., 1995) have revealed that the thinning of the crust associated with the uplift of the Adamawa region, with an abnormally hot body in the upper mantle (Gass et al., 1978; Dorbath et al., 1984; Stuart et al., 1985), could be interpreted as a continuous rise of asthenospheric material from the thinned lithosphere from the Tertiary period to the present day (Browne and Fairhead, 1983; Noutchogwé-Tatchum et al., 2006). The lithospheric seismic structure of the Central African shear zone (CASZ) has been studied in detail over the last ten years (Pasyanos and Nyblade, 2007; Priestley et al., 2008; Fishwick, 2010; Gallacher and Bastow, 2012; Koch et al., 2012; De Plean et al., 2014). These studies indicate that the mantle beneath the CCVL is characterized by low seismic wave velocities and that the lithosphere–asthenosphere boundary is about 100 km deep (~60 km).

Seismically, the central CCVL is active, particularly around Mount Cameroon and Bioko Island. Recorded events reach magnitudes up to 5 and the epicentral intensities of VII–VIII (Ateba et al., 2009; Medza Ekodo et al., 2023). This sector is therefore considered at risk, with earthquakes of low to moderate magnitude (0.5–5) but potentially high intensity, up to VIII on the Modified Mercalli scale (Thierry et al., 2008).

The northern segment of the CCVL, extending from the Adamawa Plateau to the Tibesti massif, is characterized by large volcanic massifs dominated by alkaline to peralkaline lavas derived from a metasomatized mantle source (Vicat et al., 2002; Gourgaud and Vincent, 2003; Mbowou et al., 2012; Shellnutt et al., 2016; Gountié Dedzo, Asobo, et al., 2019; Tchouhla et al., 2023).

This study examines volcanic formations from the Ziver area (Figure 1c), composed predominantly of mafic lavas (basanite, basalt, and hawaiite) and felsic lavas (trachyte and rhyolite). These lavas occur as blocky outcrops forming dome-shaped hills, as flows, or as small cones ~50 m high and 100–150 m in diameter.

3. Analytical methods

Powders and thin sections of selected rock samples were prepared at the *Geosciences Environnement Toulouse* laboratory (GET), CNRS-IRD-

CNES-University Paul Sabatier (Toulouse 3, France), for geochemical and mineralogical analyses.

Major elements minerals analyses were conducted at the *Centre de microcaractérisation Raimond Castaing*, CNRS-University Paul Sabatier (Toulouse 3, France), using a Cameca SX Five electronic microprobe. Samples were carbon-coated (15 nm thick layer, density 2.25 g/cm^3) before analysis. The conditions were accelerating voltage of 15 kV and a probe current of 10 or 20 nA (depending on mineral resistance to the electron beam).

Whole-rock major and trace element concentrations were determined at the *Service d'Analyses des Roches et des Minéraux* (SARM, CRPG, France) using an ICP-OES for major elements and an ICP-MS for trace elements analyses. New Rb/Sr and Sm/Nd isotopic analyses were performed for four (04) lava samples from Ziver including two basanites, one trachytes and one rhyolite. The Sr/Nd isotopic data were performed at GET, using the Thermo Scientific TRITON+ solid source mass spectrometer, following Labou et al. (2020) and C.-F. Li, X.-H. Li, Q.-L. Li, Guoa and Lia (2011) and C.-F. Li, X.-H. Li, Q.-L. Li, Guoa, X.-H. Li, et al. (2012) procedures. Before measurement, about 100 mg of whole rock powder was weighed in a teflon beaker and dissolved in a mixture HF/HNO_3 1:1. After dissolution, samples were diluted in 1 ml, 2% HNO_3 and Nd/Sr were extracted from the matrix (2N HNO_3) using a combination of Sr–Spec and Thru–spec Eichrom resins. Mixed Sr and REE were loaded on a Re filament and were run sequentially (first Sr then Nd) using a double Re filament protocol. Monitoring of the interferences of ^{87}Rb and ^{144}Sm was proceeded according to the protocol of C.-F. Li, X.-H. Li, Q.-L. Li, Guoa, X.-H. Li, et al. (2012) and the quality and reproducibility of the measurements were controlled using a sequential measurement of isotopic standards (SRM 987 and JNdi), doped isotopic standards (NBS 987 + Rb and JNdi + Sm) and laboratory–dedicated Sr + REE artificial solutions.

4. Results

4.1. *Nomenclature and petrography*

The volcanic rocks studied include both mafic (basanites, basalts, hawaiites) and felsic lavas (trachytes and rhyolites), classified according to the scheme of Le Bas et al. (1986) (Figure 2). Mafic volcanic rocks have a microlitic to porphyritic texture. The phenocryst phases are principally plagioclase, olivine, pyroxene and opaque minerals are the main phenocrysts. Olivine occurs in some samples and is frequently altered to iddingsite. The groundmass of these lavas consists of microlites of plagioclases alongside clinopyroxene, olivine, and oxides (Figure 3c–f). Felsic volcanic rocks are light to dark–grey, locally brecciated with fragments of the granitic basement. They have a porphyritic texture with a groundmass composed mainly of fine crystallized alkali feldspar, clinopyroxene and opaque minerals. Phenocrysts consist mainly of alkali feldspars: 10–15 vol%, clinopyroxene: 1–5 vol% and opaque minerals: 3–10 vol%. Microcrystals of opaque minerals are rounded or angular, and, for some, embedded in clinopyroxene crystals. Microliths show, in some samples, a preferred orientation underlining a magmatic fabric.

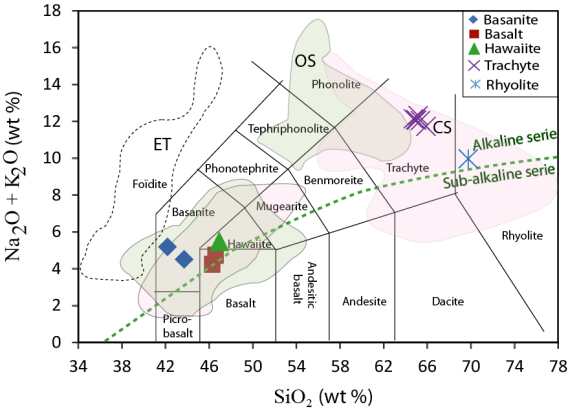

Figure 2. TAS classification diagram for Ziver lavas after Le Bas et al. (1986). The discrimination dotted line is after Irvine and Barragar (1971). Domains of the different sectors of the CCVL, as defined by Déruelle, Ngounouno, et al. (2007): CS (Continental sector); OS (Oceanic Sector), ET (Mount Etinde).

4.2. *Minerals major elements composition*

4.2.1. *Olivine*

The olivine crystals analyzed from the Ziver lavas are consistently magnesian, with compositions ranging from Fo_{70} to Fo_{92}. The corresponding Mg# values (100 × Mg/(Mg + Fe^{2+})) range from 69 to 92. Electron microprobe analyses reveal a broad range of chemical compositions, with minor element

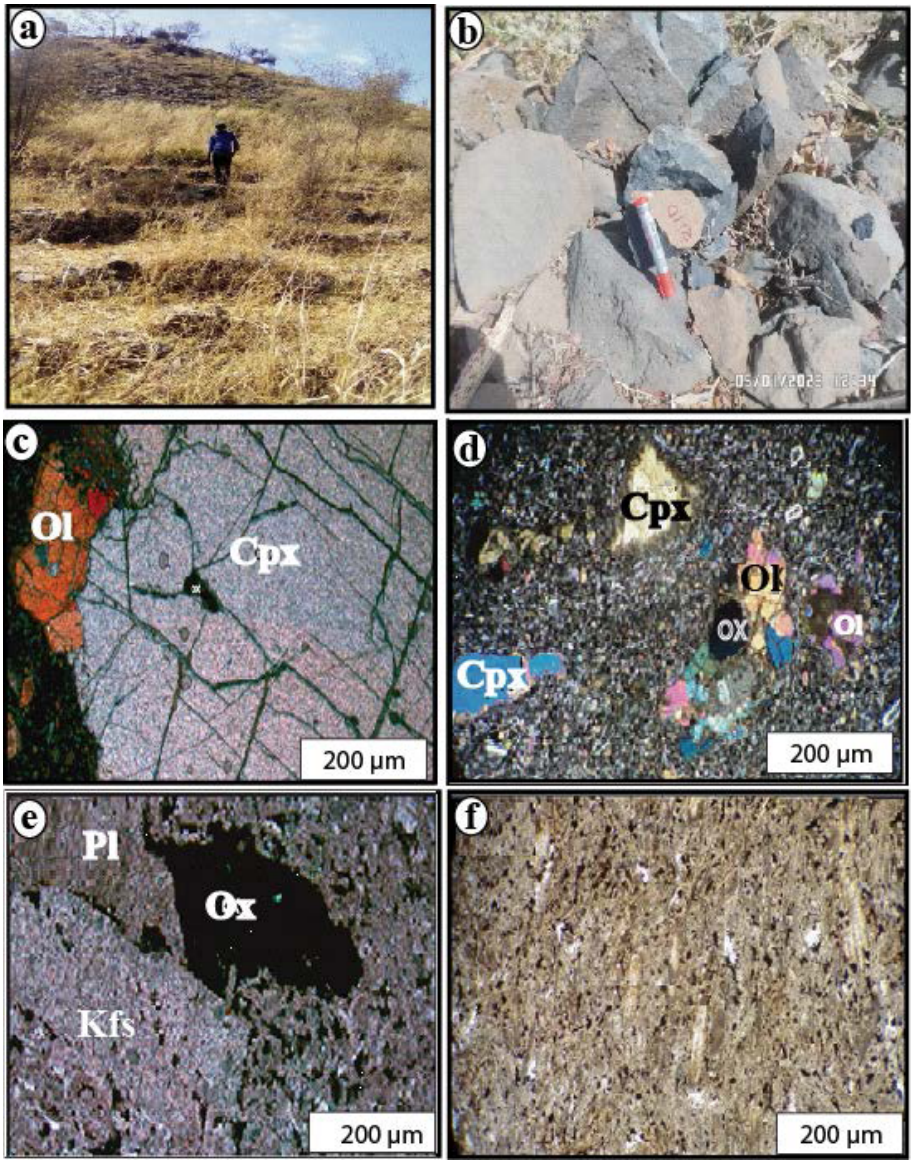

Figure 3. Field photographs and representative photomicrographs for the magmatic rocks from Ziver. (a) Basalt outcrop in the Ziver area; (b) vacuolar structure observed in basalt outcrops; (c) microlitic porphyritic texture; (d) olivine and clinopyroxene crystals exhibiting destabilization at their edges; (e) presence of an opaque mineral phase; (f) microlitic aphyric texture in rhyolite, with plagioclase microlites displaying a preferential orientation. Mineral abbreviations follow Whitney and Evans (2010).

concentrations, which include 0.07–2.19 wt% CaO, 0.05–50.25 wt% MgO, and 7.9–27.19 wt% FeO. Trace element compositions show 0.03–0.47 wt% NiO, 0.04–0.54 wt% MnO, and Cr_2O_3 concentrations ≤0.22 wt%. According to the classification scheme of Dick (1989), as presented in Figure 4a, the composition of the analyzed olivines in the basanite lavas ranges from forsterite to hyalosiderite.

4.2.2. *Clinopyroxene*

Clinopyroxene crystals from Ziver lavas are characterized by $TiO_2 \leq 3.41$ wt%, $Al_2O_3 \leq 8.13$ wt%, $Na_2O \leq 0.45$ wt%, FeO = 5.04–8.58 wt%, MgO = 12.26–49.73 wt%, CaO = 0.02–23.91 wt%, $Cr_2O_3 \leq 0.92$ wt%, and MnO = 0.04–0.14 wt%. The Al^{VI}/Al^{IV} ratio increases with differentiation, ranging from 0.11–0.13

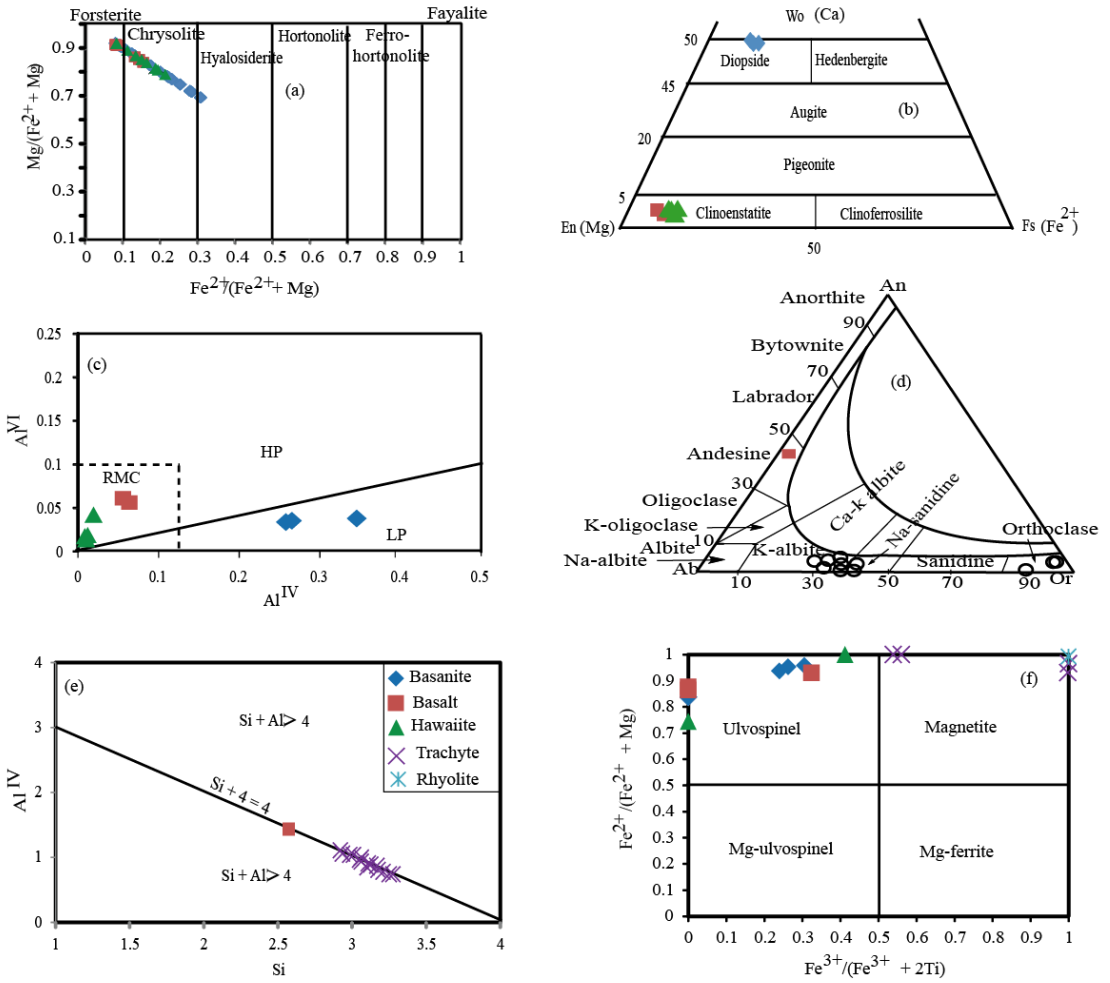

Figure 4. Mineralogical compositions of the studied lavas: (a) composition of olivines in the classification diagram of Dick (1989); (b) composition of clinopyroxenes in the Wo–En–Fs ternary diagram of Morimoto et al. (1988); (c) position of clinopyroxenes in the Al^{VI} versus Al^{IV} variation diagram of Caldeira and Munha (2002). RMC: Refractory mantle clinopyroxene fields from Jagoutz et al. (1979). HP = High pressure; LP = Low pressure; (d) composition of analyzed feldspars in the An–Ab–Or diagram of Smith and Brown (1988); (e) projection of the analyzed feldspars iin Al^{IV} versus Si diagram; (f) projection of the Fe–Ti oxides in the classification diagram of Haggerty and Tompkins (1984).

in basanite, 0.24–1.0 in basalt, and up to 2.18 in hawaiite. According to the classification of Morimoto et al. (1988) (Figure 4b), the analyzed pyroxenes correspond to clinoenstatite ($Wo_{0.02–1.13}En_{89.97–92.10}Fs_{0.00–0.38}Ac_{0–0.3}$) in basalts and hawaiites, and to diopside ($Wo_{48.90–50.02}En_{36.78–38.61}Fs_{9.76–11.50}Ac_{1.4–1.7}$) in basanites. In the Al^{VI} versus AlI^{V} discriminant diagram of Caldeira and Munha (2002), diopside plots in the low-pressure domain ($Al^{VI}/Al^{IV} < 1$), whereas clinoenstatite falls within the high-pressure RMC field defined by Jagoutz et al. (1979) for refractory mantle pyroxenes (Figure 4c).

4.2.3. *Feldspars*

Representative feldspars from Ziver lavas are chemically characterized by CaO ≤ 9.24 wt%, Al_2O_3 = 18.12–26.76 wt%, FeO = 0.05–0.25 wt%, Na_2O = 1.14–7.98 wt%, and K_2O = 0.25–15.01 wt%. In the An–Ab–Or classification diagram of Smith and Brown (1988) (Figure 4d), feldspars plot as andesine in mafic lavas, and as potassic albite, sanidine, and anorthose in felsic lavas. All feldspars show Si + $Al^{IV} \approx 4$ (Figure 4e). Structural formula calculations yield Si = 2.98–2.99 and Al = 0.99–1.02 a.p.f.u. in

mafic lavas, and Si = 2.88–3.01 and Al = 0.97–1.10 a.p.f.u. in felsic lavas.

4.2.4. *Opaque minerals*

Opaque minerals in the Ziver lavas are represented by ulvöspinel in the mafic rocks and magnetite in the felsic rocks (Figure 4f), following the classification of Haggerty and Tompkins (1984). In felsic lavas, FeO contents (49.89–88.60 wt%) are consistently higher than TiO_2 (2.89–50.08 wt%), whereas in mafic lavas TiO_2 (36.88–41.70 wt%) exceeds FeO (34.64–36.61 wt%). The Cr# [100·Cr/(Cr + Al)] varies from 0 to 26.46 in the mafic lavas and from 0 to 7.73 in the felsic lavas.

4.3. *Whole-rock geochemistry*

The geochemical study is based on bulk-rock major and trace elements analysis of twelve (12) representative lava samples and four (04) Rb/Sr and Sm/Nd isotopic ratios (Table 1). The laboratory bulk data were recalculated on an anhydrous basis because some samples displayed loss on ignition greater than the critical value of 2 wt%. The differentiation index [DI = quartz + albite + orthoclase or (Nepheline + Leucite + Albite + orthoclase)] of these samples ranges from 24.45 (basanite Zi10) to 90.13 (rhyolite M29). A compositional gap is noticed between 47.04 and 64.65 wt% SiO_2 contents.

4.3.1. *Major elements*

The major-element compositions of the Ziver lavas are characterized by TiO_2 ranging from 0.02 to 4.11 wt%, Al_2O_3 from 12.70 to 16.13 wt%, Fe_2O_3 from 4.96 to 13.89 wt%, Na_2O from 2.61 to 7.09 wt%, and K_2O from 1.40 to 5.18 wt%, with Na_2O/K_2O ratios between 1.00 and 2.25, and Mg# values [(100·MgO/(MgO + FeOt)] varying from 1.52 to 72.57. Mafic lavas contain normative apatite ranging from 1.39 to 3.10 wt% and nepheline from 2.00 to 12.03 wt%, whereas felsic lavas are characterized by normative quartz ranging from 1.62 to 18.20 wt% and hypersthene from 5.04 to 7.97 wt%.

In Harker variation diagrams (Figure 5), MgO, Fe_2O_3, CaO, P_2O_5, and TiO_2 contents of the studied lavas, taken together with published data of northern CCVL lavas, decrease systematically with increasing SiO_2, contrary to Na_2O and K_2O, which increase from mafic to felsic compositions. Al_2O_3 contents increase in mafic lavas and decrease in felsic lavas while MnO shows no significant variation.

4.3.2. *Trace elements*

The concentrations of several trace elements, including Ni, Cu, Cr, V, and Sr, decrease markedly from mafic to felsic lavas. Nickel ranges from 16.93 to 435.58 ppm, with the highest contents recorded in mafic lavas. Co varies from 2.56 to 61.96 ppm, Cr from 92.82 to 717.16 ppm, and V from 1.45 to 241.03 ppm, all showing a progressive decrease from basalts to trachytes. Sr contents range from 767.8 to 1678.3 ppm in mafic lavas and from 14.6 to 27.81 ppm in felsic lavas. In contrast, the concentrations of Y, Pb, Ga, Nb, Rb, and La generally increase from mafic to felsic lavas. Y increases from 17.9 ppm in basalt sample Zi16 to 124.2 ppm in rhyolite M29; Pb ranges from 1.77 ppm in sample M33 to 19.98 ppm in rhyolite M29; Hf increases from 4.08 ppm in sample Zi10 to 34.36 ppm in sample M29; and U ranges from 0.77 ppm in sample M33 to 7.28 ppm in trachyte Zi8 (Table 1). The distribution of trace elements (V, Cu, Cr, Ni, Sr, Pb, Nb, and Ta) as a function of SiO_2 content (Figure 6) shows that the Ziver lavas plot in the same fields with previously studied lavas from the northern segment of the CCVL, and therefore exhibit the similar geochemical characteristics. For example, all compatible elements (Cr, Ni and V) show a systematic decrease with increasing SiO_2. Conversely, incompatible elements such as Nb, Ta, Pb, and Sr show a general trend of increasing or remaining relatively stable with silica.

The primitive mantle normalized multi-element patterns show that Ziver lavas exhibit geochemical signatures remarkably consistent with those described for volcanoes in the northern segment of the CCVL (Ngounouno, Déruelle and Demaiffe, 2000; Rankenburg et al., 2005; Gountié Dedzo, Asobo, et al., 2019; Tchouhla et al., 2023; Djerossem et al., 2024). Mafic lavas (Figure 7a) show a marked enrichment in highly incompatible elements (LILE and HFSE), notably Cs, Rb, Ba, Th, U, Nb, Ta, K, and La, as well as a gradual decrease in heavy rare earth element (HREE) contents. This distribution, characterised by a generally convex curve and an absence of significant anomalies in Nb–Ta or Ti, closely corresponds to the spectrum of oceanic intraplate basalts (OIB) described by Sun and McDonough (1989).

Table 1. Whole rock chemical composition of lavas from Ziver

Rock type	Basanite		Basalt		Hawaiite			Trachyte				Rhyolite
Sample ID	M33	Zi10	Zi16	M20	Zi17	Zi14	Zi7	Zi12	Zi5	Zi11	Zi8	M29
SiO_2	42.10	43.55	45.63	45.78	46.01	63.16	63.52	63.58	63.66	63.92	64.28	70.10
Al_2O_3	13.38	12.07	12.95	13.90	15.19	15.63	15.72	15.53	15.78	16.14	15.76	13.79
Fe_2O_3	13.90	12.29	11.13	11.20	11.07	5.24	5.23	5.57	5.41	5.54	5.19	5.53
MnO	0.18	0.19	0.15	0.16	0.15	0.17	0.19	0.17	0.19	0.10	0.15	0.22
MgO	9.17	13.90	13.10	10.55	8.04	0.06	0.08	0.08	0.04	0.13	0.09	0.00
CaO	10.46	10.19	8.34	8.94	8.70	1.16	1.12	1.22	1.30	0.14	0.98	0.04
Na_2O	3.56	3.05	2.62	2.94	3.34	6.52	6.57	6.09	6.71	5.46	7.10	5.57
K_2O	1.58	1.40	1.42	1.45	1.71	5.18	5.16	5.12	5.17	5.41	4.99	4.22
TiO_2	4.11	2.38	2.52	2.72	2.85	0.20	0.20	0.20	0.20	0.20	0.21	0.26
P_2O_5	1.32	0.59	0.57	0.63	0.74	0.00	0.00	0.00	0.00	0.00	0.00	0.00
Sum	100.08	100.22	99.01	99.57	98.98	98.93	99.41	99.37	99.86	98.90	99.78	100.71
Mg#	59.74	71.77	72.57	67.91	62.01	2.63	3.41	3.20	1.52	4.94	3.79	0.00
ID	29.42	24.45	28.90	30.95	35.26	84.15	84.67	85.38	84.51	85.76	85.25	90.13
CIPW norm												
Quartz	0.00	0.00	0.00	0.00	0.00	2.05	2.09	3.85	1.62	7.90	2.52	17.07
Orthoclase	8.40	9.46	8.61	8.79	10.41	31.62	31.32	31.14	31.20	33.10	30.02	24.67
Albite	4.81	8.37	19.05	20.06	22.25	53.22	53.59	52.97	53.44	47.83	54.19	48.95
Anorthite	15.33	16.10	19.89	21.05	22.11	0.00	0.00	0.00	0.00	0.73	0.00	0.15
Nepheline	11.60	12.03	2.00	2.96	3.76	0.00	0.00	0.00	0.00	0.00	0.00	0.00
Diopside	25.77	22.55	15.04	16.37	14.16	5.26	5.06	5.54	5.88	0.00	4.39	0.00
Hypersthene	0.00	0.00	0.00	0.00	0.00	5.23	5.36	5.08	5.04	7.97	5.53	7.67
Olivine	25.97	18.03	27.17	21.96	17.97	0.00	0.00	0.00	0.00	0.00	0.00	0.00
Magnetite	2.15	2.43	1.97	1.99	1.97	0.00	0.00	0.94	0.00	0.99	0.00	0.97
Ilmenite	4.59	7.92	4.92	5.32	5.60	0.39	0.39	0.40	0.38	0.39	0.40	0.46

(continued on next page)

Table 1. (continued)

Rock type	Basanite		Basalt		Hawaiite			Trachyte				Rhyolite
Apatite	1.39	3.10	1.36	1.50	1.77	0.00	0.00	0.00	0.00	0.00	0.00	0.00
Sum	100.00	100.00	100.00	100.00	100.00	100.00	100.00	100.00	100.00	100.00	100.00	100.00
Trace elements (ppm)												
Co	51.14	59.04	54.08	52.38	42.97	1.30	0.58	2.49	0.72	0.71	1.10	0.34
Cr	534.55	717.16	454.66	429.23	240.18	185.59	92.83	351.17	117.99	96.60	147.24	62.10
Cu	61.97	50.66	46.41	47.87	31.32	6.98	3.90	11.86	3.97	4.94	6.42	4.20
Ni	265.72	422.58	435.58	348.53	142.44	85.16	25.91	179.26	34.72	47.19	54.25	8.30
V	241.03	201.40	176.73	191.00	185.85	1.69	1.45	2.10	1.45	0.00	1.71	5.80
Cs	0.17	0.36	0.27	0.29	0.32	0.40	0.28	0.26	0.50	0.37	0.46	0.34
Rb	19.69	34.63	22.40	28.49	28.00	115.46	108.27	106.25	115.63	132.08	130.39	130.00
Ba	491.75	403.43	343.75	409.75	446.10	93.16	111.54	104.04	161.79	99.26	34.64	152.00
Th	2.75	4.30	3.21	4.04	4.48	13.78	14.25	14.18	14.19	14.57	22.03	28.90
U	0.77	1.11	0.93	1.15	1.32	3.51	2.12	1.66	3.55	1.74	7.28	4.36
Nb	56.10	51.98	42.42	48.74	56.54	121.64	129.99	119.57	125.97	125.65	182.21	239.00
Ta	3.92	3.66	2.94	3.51	4.05	8.76	8.98	8.81	8.78	9.36	13.51	17.90
K	46.52	52.37	47.15	48.05	56.62	172.07	171.28	169.85	171.74	179.54	165.80	140.13
La	44.29	35.91	31.79	37.73	43.61	127.39	128.59	127.53	126.93	92.10	156.46	149.00
Ce	96.94	70.54	65.23	76.54	87.40	254.60	258.66	256.22	255.27	272.80	303.63	310.00
Pb	1.77	2.38	1.94	2.40	2.31	10.04	10.06	10.11	10.09	10.33	9.64	20.80
Pr	12.18	8.34	7.84	9.28	10.33	29.13	29.71	29.29	29.19	24.44	33.56	34.40
Sr	1678.29	767.84	911.30	1191.63	1291.19	24.76	16.35	53.36	27.81	14.58	15.08	23.80
Nd	51.45	33.40	32.17	37.94	41.12	109.17	112.15	108.48	109.94	96.47	118.30	128.00
P	26.48	59.25	25.59	28.28	33.22	46.91	47.89	46.81	47.47	49.06	48.50	61.49
Sm	10.19	6.92	6.73	7.65	8.23	20.83	21.26	20.78	21.07	21.78	21.53	27.30
Hf	4.55	4.08	4.58	5.35	5.92	22.25	22.04	22.51	22.22	20.58	32.51	37.90

(continued on next page)

Table 1. (continued)

Rock type	Basanite		Basalt		Hawaiite			Trachyte				Rhyolite
Zr	197.95	175.18	208.69	243.28	282.42	1123.58	1048.73	1102.96	1073.28	932.28	1667.70	1619.00
Eu	3.55	2.27	2.21	2.55	2.67	3.71	3.80	3.72	3.78	3.83	1.42	4.49
Gd	8.07	5.87	5.46	6.24	6.52	17.07	17.77	17.22	17.19	18.95	17.30	25.70
Tb	1.07	0.83	0.74	0.85	0.90	2.56	2.64	2.60	2.57	2.81	2.65	4.10
Dy	5.55	4.53	4.04	4.53	4.79	14.50	14.93	14.76	14.57	15.94	15.37	25.00
Ho	0.94	0.83	0.71	0.81	0.85	2.74	2.84	2.82	2.78	3.04	2.98	5.08
Y	22.97	20.57	17.90	20.75	21.24	69.89	70.38	70.89	69.79	75.44	75.20	130.00
Er	2.13	1.98	1.66	1.89	1.97	6.98	7.13	7.21	7.03	7.59	7.75	13.70
Tm	0.26	0.26	0.22	0.25	0.26	0.99	1.02	1.02	1.01	1.09	1.15	2.08
Yb	1.50	1.52	1.27	1.46	1.50	6.15	6.33	6.35	6.16	6.65	7.33	12.70
Lu	0.21	0.21	0.18	0.21	0.21	0.90	0.93	0.92	0.91	0.97	1.08	1.70
Isotopes												
$^{87}Sr/^{86}Sr$ mes	0.70362	0.70311							0.71856			0.71798
$2\sigma \times 10^{-6}$	4	5							5			7
$^{143}Nd/^{144}Nd$ mes	0.512913	0.512949							0.512763			0.512833
$2\sigma \times 10^{-6}$	0.000003	0.000005							0.000006			0.000005
$^{145}Sm/^{144}Nd$	0.34841	0.34841							0.34841			0.34842
$2\sigma \times 10^{-6}$	1	4							4			3
$^{87}Rb/^{86}Sr$	0.03294	0.12667							11.6964			15.4293
$^{147}Sm/^{144}Nd$	0.11562	0.120932							0.111854			0.132268
$(^{87}Sr/^{86}Sr)_i$	0.703614	0.709718							0.720302			0.712068
$(^{143}Nd/^{144}Nd)_i$	0.512893	0.512017							0.512816			0.512810

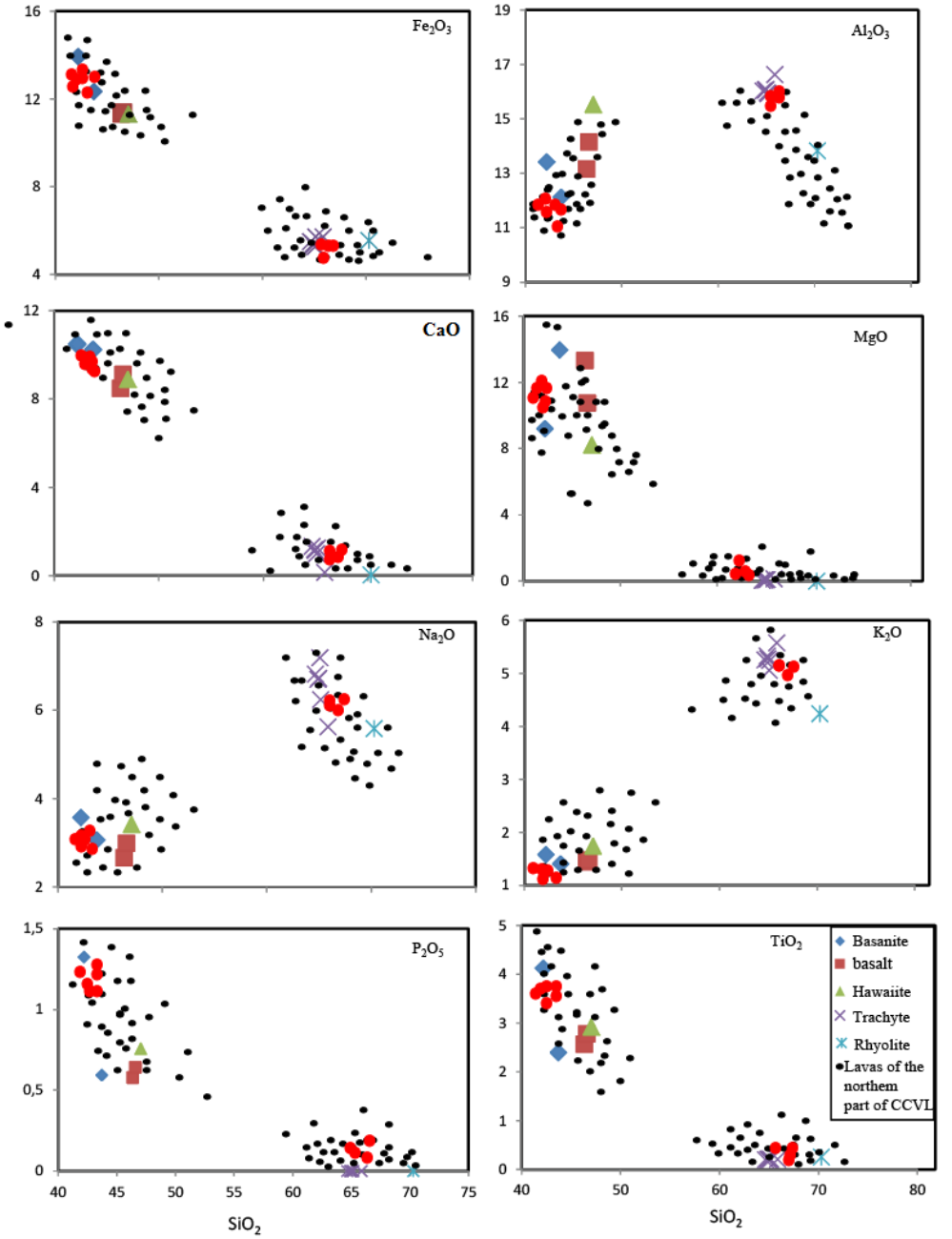

Figure 5. Variation of major elements (Fe_2O_3, Al_2O_3, CaO, MgO Na_2O, K_2O, P_2O_5 and TiO_2) as a function of the SiO_2 in the studied lavas, together with other lavas from northern CCVL. Data sources of the lavas from the northern part of the CCVL are from Ngounouno, Déruelle and Demaiffe (2000), Rankenburg et al. (2005), Gountié Dedzo, Asobo, et al. (2019), Tchouhla et al. (2023) and Djerossem et al. (2024). The red dots represent the lava closest to our study area.

The felsic lavas of Ziver (Figure 7b), represented by trachytes and rhyolites, retain the enriched general structure observed in mafic lavas, but are accentuated by higher normalisation factors, a direct consequence of their advanced differentiation. These lavas show: (i) a marked enrichment in incompatible elements (LILE and LREE) indicating strong magmatic differentiation, (ii) a clear negative

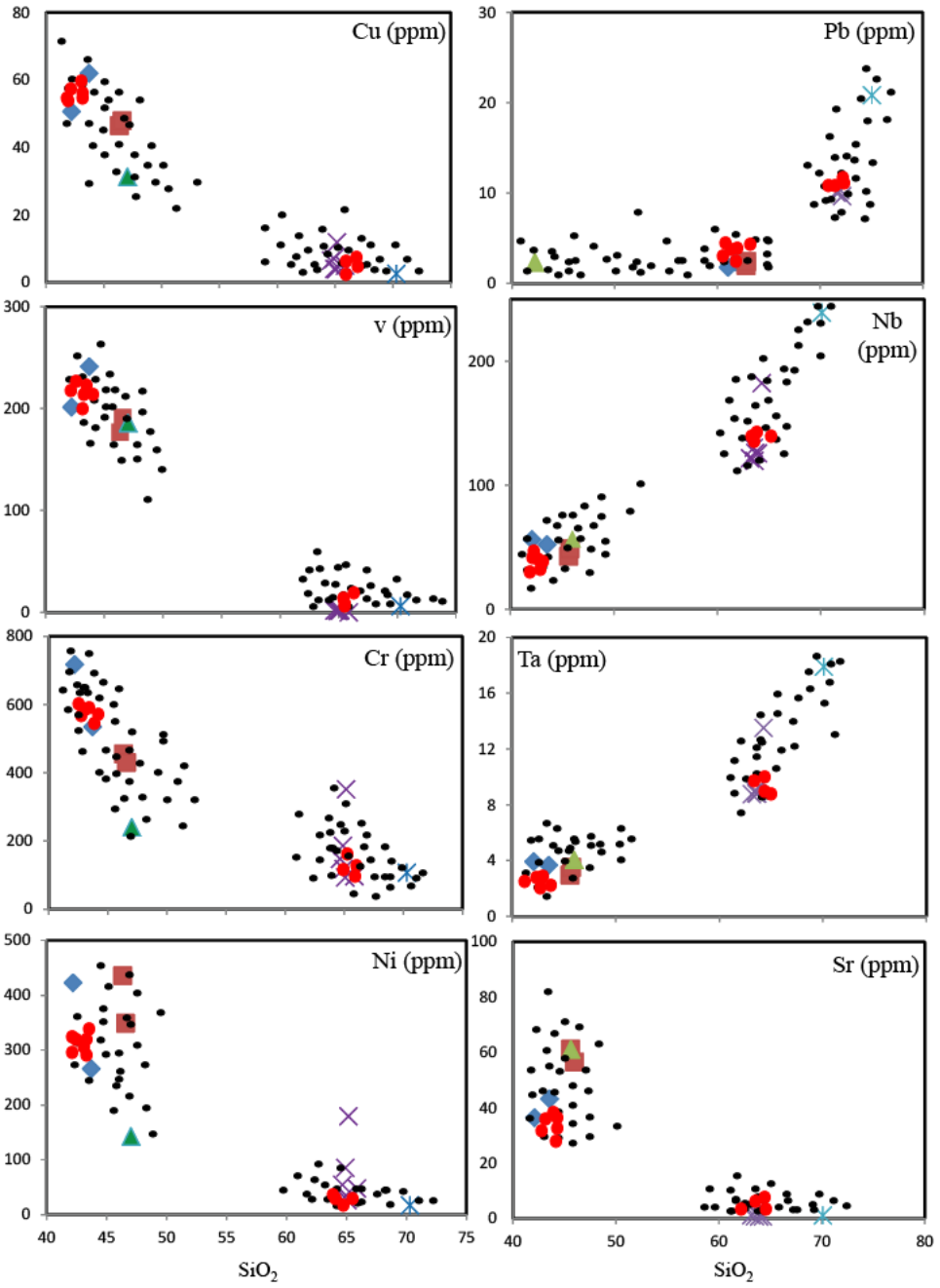

Figure 6. Distribution of traces elements (V, Cu, Cr, Ni, Sr, Pb, Nb and Ta) versus SiO_2 content in lavas from Ziver are. Data sources of the northern part of the CCVL, and Symbols are the same in Figure 5.

anomaly in Eu, linked to plagioclase fractionation, typical of evolved magmas, and (iii) a relative depletion in HREE, but less marked than in basalts, indicating melting at shallower depths, without major influence on garnet.

The chondrite-normalised rare earth element spectra show that the mafic lavas of Ziver (Figure 8a) have moderately sloping profiles, characterised by a strong enrichment in LREE and a gradual decrease towards HREE. This geometry is almost parallel to the

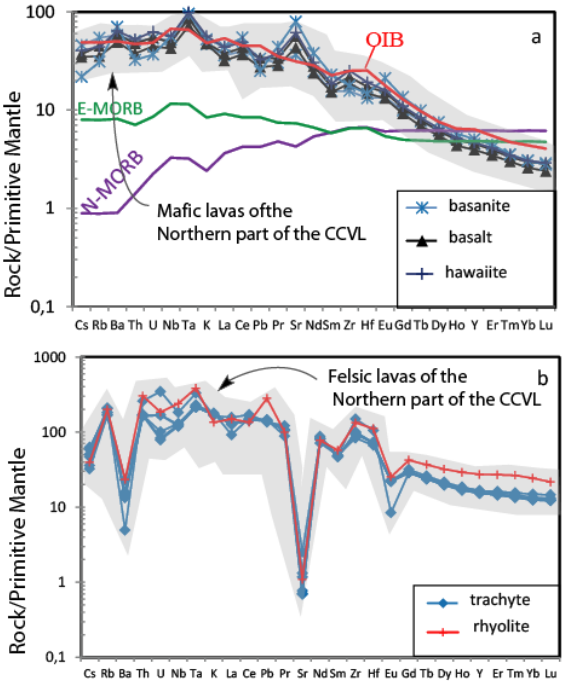

Figure 7. Primive mantle-normalized multi-element spider diagrams for Ziver lavas: (a) mafic lavas and (b) felsic lavas. Primitive mantle composition is after McDonough and Sun (1995). Data for OIB, N-MORB, and E-MORB are from Sun and McDonough (1989). Data sources of the northern part of the CCVL are the same used in Figure 6.

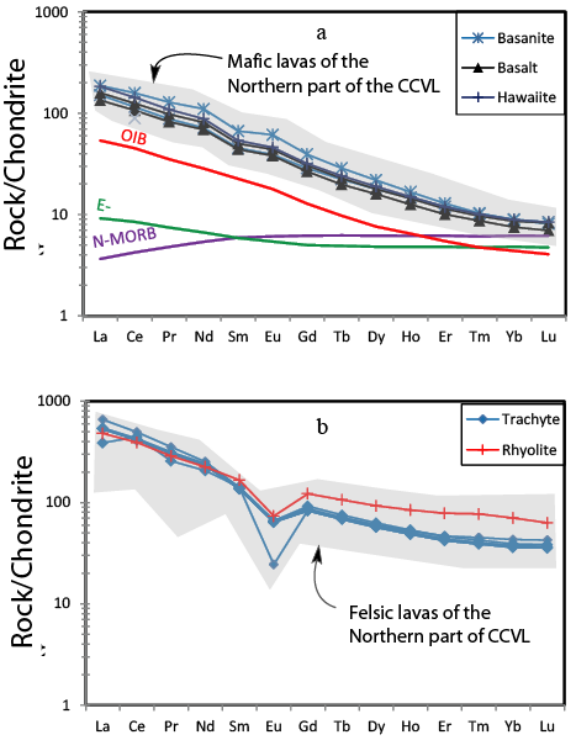

Figure 8. Chondrite-normalized REE patterns for Ziver lavas: (a) mafic lavas and (b) felsic lavas. Chondrite values are from McDonough and Sun (1995). Data for OIB, N-MORB, and E-MORB are from Sun and McDonough (1989).

OIB spectra and clearly distinct from the N-MORB or E-MORB signatures. There are no significant anomalies in Eu or Ce. This enrichment in light rare earth elements is marked by the high $(La/Yb)_N$ ratio (15.19–20.91) and the gradual decrease in MREE with a ratio (Gd/Yb) (3.19–4.44). Depletion of medium and heavy rare earth elements is evidenced by $(La/Sm)_N$ ranging from 2.4 to 4.6 and $(Dy/Yb)_N$ from 1.32 to 1.61, respectively. The Ziver mafic lavas show a slight positive Eu anomaly. Felsic lavas retain an overall enriched pattern similar to that of mafic lavas, but with higher LREE contents, reflecting their more advanced degree of evolution. The presence of moderate negative anomalies in Eu can be explained by the fractional crystallisation of plagioclase during the late stages of magmatic evolution (Figure 8b).

4.4. *Sr–Nd isotopes*

Four new Sr and Nd isotopic ratios were obtained both in mafic (basanite) and felsic (trachyte, rhyolite) lavas. Calculations for major elements were performed on an anhydrous basis. Isotopic data were corrected to 40 Ma, an age derived from nearby rhyolites on the Kapsiki plateau (Ngounouno, Déruelle and Demaiffe, 2000), due to their geospatial proximity to the Ziver area.

The $^{87}Sr/^{86}Sr$ isotopic ratios range from 0.70311 in the basanite Zi10 to 0.71856 in the trachyte Zi5, while the $^{143}Nd/^{144}Nd$ ratios vary between 0.51295 and 0.51276, respectively. The $(^{87}Sr/^{86}Sr)_{initial}$ varies from 0.70361 (basanite Zi10) to 0.71207 (trachyte Zi5), and $(^{143}Nd/^{144}Nd)_{initial}$ ranges from 0.51282 (trachyte Zi5) to 0.51202 (basanite Zi10), with initial εNd values varying from 3.86 (trachyte Zi5) to 7.44 (basanite Zi10).

5. Discussion

5.1. *Petrogenesis of lavas*

The coherence of trace-element patterns across the studied lavas suggests a genetic relationship,

indicating that they belong to the same magmatic series despite the presence of a compositional gap. This gap, which is characteristic of the Ziver lavas, emphasizes their bimodal nature-a feature also documented in several other continental volcanic massifs along the CCVL, including Nganha (Nono et al., 1994), Bambouto, Oku, and Ngaoundéré (Marzoli, Renne, et al., 1999), the Kapsiki Mountains (Ngounouno, Déruelle and Demaiffe, 2000), the Benue Trough (Ngounouno, Déruelle, Demaiffe and Montigny, 2003), the Bamenda Mountains (Kamgang, Njonfang, et al., 2010), Mbengwi (Mbassa et al., 2012), and Tchabal Gangdaba (Itiga et al., 2013).

Several geochemical criteria support a mantle-derived origin and subsequent evolutionary differentiation of these magmas. The basanites, interpreted as the most primitive lavas in the suite, are marked by high Ni contents (265.72–422.58 ppm) and elevated Mg# values (59.74–71.77), consistent with crystallization from an undifferentiated, mantle-derived mafic magma.

The major variation diagrams show that the lavas from the Ziver area follow the same evolutionary trends as those from the northern part of the CCVL, characterised by an alkaline series controlled by fractional crystallisation of mafic phases and plagioclase. The basic compositions overlap closely, indicating a common mantle source. However, Ziver exhibits more dispersed intermediate to differentiated compositions, as well as more evolved terms (trachytes–rhyolites), suggesting more advanced differentiation and locally distinct magmatic evolution conditions within the CCVL.

Overall, the Ziver lavas closely overlap with the geochemical fields defined for the volcanoes of the northern CCVL (Ngounouno, Déruelle and Demaiffe, 2000; Rankenburg et al., 2005; Gountié Dedzo, Asobo, et al., 2019; Tchouhla et al., 2023; Djerossem et al., 2024; Djamilatou et al., 2025). Their composition indicates a mantle source analogous to that of other edifices in the area and some evolution dominated by fractional crystallisation, with no significant crustal input. These results indicate that the Ziver volcanism represents an additional coherent segment of the regional magmatic field, extending the petrogenetic processes defined for the northern part of the CCVL.

Normative mineralogy further constrains their silica saturation state: the mafic lavas are silica-undersaturated, as indicated by the presence of normative nepheline, reaching up to 12.03 vol% in sample M33. This high nepheline content underscores their pronounced alkaline affinity. In contrast, the felsic lavas are silica-oversaturated, with SiO_2 contents ranging from 64.66 to 70.30 wt% and containing normative quartz (1.62–18.20 vol%) and hypersthene (5.04–7.97 vol%). Their peralkaline index [$(Na_2O + K_2O)/Al_2O_3$] varies from 0.92 to 1.08, reflecting the peralkaline nature of the felsic lavas. The combination of high SiO_2 contents and peralkaline character is a diagnostic feature of evolved alkaline magmas.

5.2. *Nature of the source(s) of the Ziver volcanic rocks*

The chemical composition of the mantle source can be constrained using incompatible element ratios (e.g., Nb/Ta, Nb/U, Ta/U), which remain relatively stable during magmatic differentiation. The Nb/Ta, Nb/U, and Ta/U ratios of the mafic lavas (0.79–0.82, 1.24–2.14, and 0.71–0.81, respectively) closely match those of the felsic lavas (0.77–0.82, 1.02–2.75, and 0.76–1.10, respectively), supporting a cogenetic relationship between the two series. Both groups are enriched in incompatible elements, consistent with derivation from relatively low degrees of partial mantle melting. Their $(Ce/Yb)_N$ ratios (5.56–17.94) partly overlap the range defined by Déruelle, Ngounouno, et al. (2007) for the continental sector of the CCVL (12–22; average ≈ 15) and are similar to values reported for the Kapsiki Plateau ($(Ce/Yb)_N \approx 14.3$; Ngounouno, Déruelle and Demaiffe, 2000). These comparatively low ratios, combined with strong enrichment in light rare earth elements (LREE), point toward low to moderate degrees of mantle melting.

The almost complete overlap of the Ziver lavas with the geochemical fields established for neighbouring edifices north of the CCVL (Gawar: Gountié Dedzo et al., 2019; Mokolo Hossehone: Tchoulha et al., 2023; Rankenburg et al., 2005, Kapsiki: Ngounouno et al., 2000; (Djamilatou et al., 2025), Iriba: Djerossem et al., 2024) highlights regional homogeneity in the nature of the mantle source and in the differentiation processes. The data confirm that the Ziver magmas derive from an OIB-type enriched mantle source, having undergone

progressive differentiation controlled mainly by fractional crystallisation, without a major crustal contribution. This pattern reinforces the idea that Ziver volcanism is a further expression of the intraplate alkaline magmatism characteristic of the CCVL.

Additional constraints on mantle source characteristics are provided by the Gd/Yb versus La/Yb and Sm/Yb versus La/Sm diagrams (Figure 9), combined with partial melting models for lherzolite with homogeneous compositions (Yokoyama et al., 2007). In these diagrams, the Ziver samples fall along the melting trajectories of garnet-bearing peridotite, implying magma generation at depths consistent with the stability of the garnet in the residue (~70–80 km). This is further confirmed by very high $(La/Yb)_N$ ratios (15.19–20.91) and Gd/Yb (3.19–4.44), typical of magmas resulting from the melting of a garnet-bearing mantle. Elevated Sm/Yb, Gd/Yb, La/Yb, and La/Sm ratios indicate very low degrees of partial melting (0.5–3%) of a garnet-bearing enriched mantle source (Figure 9), involving metasomatized lithospheric mantle and/or plume-derived enriched domains. This limited degree of melting explains the pronounced enrichment of incompatible elements, particularly LREE, which is a hallmark of OIB-type magmas. The Ziver lavas therefore share geochemical affinities with other volcanic centers of the CCVL, including Mt. Cameroon (Asaah et al., 2015), and Mokolo-Kossehone (Tchouhla et al., 2023), Mbengwi (Mbassa et al., 2012), Gawar and Zamaï (Gountié Dedzo, Asobo, et al., 2019), Iriba (Djerossem et al., 2024), and the Kapsiki Plateau (Ngounouno, Déruelle and Demaiffe, 2000). Slight variations in melting degree and depth of generation likely reflect small-scale heterogeneities in the mantle source but overall confirm the existence of a common deep mantle reservoir beneath the CCVL.

The Nb/Y versus Zr/Y diagram of Condie (2005) (Figure 10) further supports this interpretation: the Ziver lavas plot above the ΔNb line, within the plume-derived enriched mantle domain defined by Fitton, Saunders, et al. (1997). Their geochemical signature is characteristic of intraplate alkaline basalts, comparable to OIBs, and consistent with derivation from an enriched asthenospheric mantle plume source. Isotopic data ($^{143}Nd/^{144}Nd$ versus $^{87}Sr/Sr^{86}$; Foucarde, 1998) show that the basanites fall along the mantle array within the depleted mantle (DM) field,

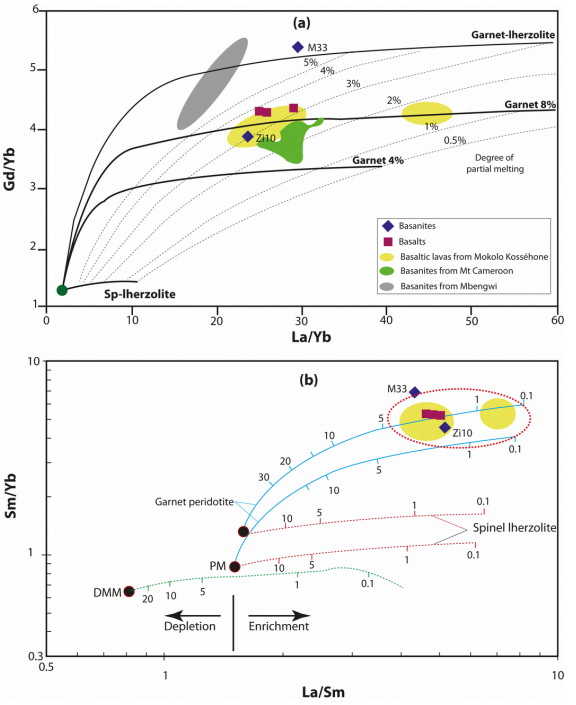

Figure 9. Gd/Yb versus La/Yb diagram illustrating the partial melting of the Ziver and Mount Cameroon basaltic lavas. The breakdown of the Mount Cameroon zone is from Yokoyama et al. (2007). The two curves marked Grt 4% and 8% represent the garnet content of the source. Calculations of garnet grades in the source were made using the partition coefficients of Halliday, Davidson, et al. (1990); (b) plot of the Ziver lavas in the Sm/Yb versus La/Sm diagram after Gurenko et al. (2006). The red dotted line field is that of basaltic lavas from northern Cameroon. Values of DMM (Depleted MORB Mantle) are from Workman and Hart (2005). Values of PM are from Sun and McDonough (1989). The different curves represent the partial melting of garnet and spinel peridotites. The gradations represent the different melting rates.

suggesting minimal crustal contamination. By contrast, the more evolved trachytes and rhyolites display enrichment in radiogenic Sr, indicating the assimilation of the upper continental crust during their evolution.

Taken together, these data indicate that the Ziver lavas were generated by the upwelling of a mantle plume in a post-orogenic intraplate setting, possibly linked to late-stage rifting. This model is consistent with both the OIB-like isotopic signatures observed in other CCVL volcanic centers and geodynamic models that invoke deep mantle upwelling beneath Central Africa.

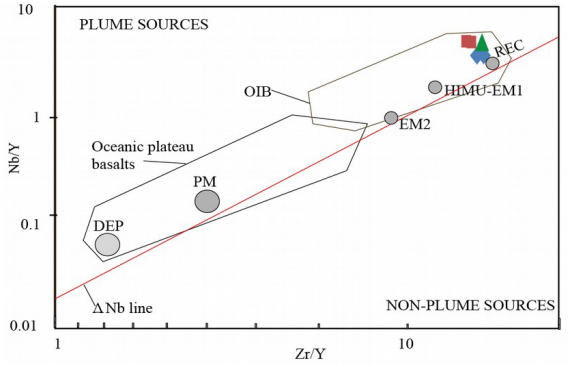

Figure 10. Tectonic setting of Ziver mafic lavas in relation to various mantle components and basalt fields, as defined by Weaver (1991) and Condie (2005). DEP = Deeply Depleted Mantle; REC = Recycled Component; PM = Primitive Mantle, DM =: depleted mantle, HIMU = high-μ, EM = Enriched mantle.

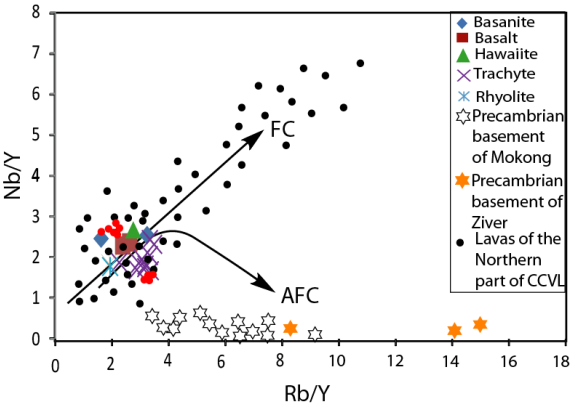

Figure 11. Position of the studied lavas in the Nb/Y versus Rb/Y diagram of Cox and C. J. Hawkesworth (1985) and Leeman and C. Hawkesworth (1986). Data for Precambrian basement are from Tchameni et al. (2016). Data sources from the northern part of the CCVL are similar to Figure 6.

5.3. *Magma differentiation processes and crustal contamination*

To better constrain the geochemical characteristics of the Ziver volcanic rocks we investigated the potential interactions between molten rocks and crustal rocks during the ascent of magma to the surface, since crustal contamination is an effective means of modifying the composition of trace elements (McDermott et al., 2005; Zellmer et al., 2005). Although not consistently observed, previous studies have already suggested that contamination of primary magmas by continental crust is significant along the CCVL (Halliday, Dicken, et al., 1988; Marzoli, Renne, et al., 1999; Rankenburg et al., 2005; Kamgang, Njonfang, et al., 2010; Kamgang, Chazot, et al., 2013; Njonfang, Tchuenté, et al., 2013; Tchuimegnie Ngongang et al., 2015). The influence of the basement on the composition of magmas can be confirmed by trace element ratios. Crustal rocks and melts derived from them are characterized by higher Rb/Nb ratios, whereas alkaline basaltic magmas are relatively enriched in Nb and therefore have a relatively low Rb/Nb ratio (Weaver and Tarney, 1984). Consequently, the low Rb/Nb ratios (0.49–1.05) observed in the basaltic rocks of Ziver are compatible with the absence or very low crustal contamination.

Furthermore, the Ziver basanites display primitive mantle–normalized trace element patterns similar to those of uncontaminated OIBs (Figure 7a), consistent with observations reported for other lavas of the CCVL (Marzoli, Piccirillo, et al., 2000; Rankenburg et al., 2005; Yokoyama et al., 2007; Aka et al., 2009; Kamgang, Chazot, et al., 2013; Asaah et al., 2015). The positive Nb–Ta anomaly in the Ziver basanite lavas is consistent with the presence of peridotite xenoliths observed in most basanites of the study area, suggesting rapid magma ascent to the surface and ruling out significant crustal contamination. In contrast, the differentiated Ziver lavas (trachytes and rhyolites) display a negative Nb–Ta anomaly (Figure 7b), indicating limited magma–crust interaction.

The Nb/Y versus Rb/Y diagram of Cox and C. J. Hawkesworth (1985) and Leeman and C. Hawkesworth (1986) is indeed generally used to assess the influence of crustal contamination on the chemical composition of the magma shown in Figure 11. The lavas studied are grouped into a domain characteristic of poorly differentiated alkaline magmas, with moderate Nb/Y ratios (1–3) and low to moderate Rb/Y ratios (1–4). Their position is close to that of the basanites, basalts, and hawaiites of the CCVL, indicating a mantle signature similar to that of Pan-African alkaline volcanism.

The black cloud representing regional data shows an upward trend (increase in Nb/Y) consistent with fractional crystallisation from a parental basanitic magma. The Ziver lavas follow this trend, suggesting that they derive from a parent magma common to the northern CCVL. The red dot (the lava

closest to Ziver) overlaps with the field of undersaturated alkaline magmas of the CCVL, supporting a direct petrogenetic link. The Precambrian basement samples (Mokong and Ziver) show low Nb/Y values (≤0.5) and higher Rb/Y values, characteristic of a crustal substrate enriched in incompatible elements. None of the lava samples show a clear trend towards these compositions, indicating limited crustal assimilation. Overall, their trace element distributions are consistent with mantle-derived alkaline magmatism that evolved in a closed system through fractional crystallization. This supports an intraplate tectonic setting involving an enriched deep-mantle source with limited crustal interaction, similar to that inferred for other volcanic centers of the CCVL, such as the Adamaoua Plateau (Nkouandou et al., 2010; Fagny et al., 2020; Mebara et al., 2022; Dili-Rake et al., 2022); the Gawer and Zamaï lavas (Gountié Dedzo, Asobo, et al., 2019); the Kapsiki plateau lavas (Ngounouno, Déruelle and Demaiffe, 2000; Djamilatou et al., 2025); the Iriba lavas in Chad (Djerossem et al., 2024).

6. Conclusions

The Ziver volcanic area includes both mafic (basanite, basalt, and hawaiite) and felsic lavas (trachyte and rhyolite), defining a bimodal series with a Daly gap between 47 and 64.7 wt% SiO_2. The geochemical data obtained on Ziver lavas show that this volcanic center is fully integrated into the magmatic dynamics of the northern segment of the CCVL. The trends in trace elements, the distribution of multi-element diagrams and rare earth spectra normalised to the primitive mantle and chondrites respectively reveal signatures typical of intraplate alkaline magmatism derived from an OIB-type enriched mantle source. The absence of negative anomalies in Nb–Ta or Ti, combined with systematic enrichment in LILE, HFSE, and LREE, rules out significant crustal input and indicates that the magmas originated from a moderately heterogeneous mantle, similar to that feeding the other volcanic edifices in the northern part of the CCVL. These studies reveal a deep, enriched mantle origin for the Ziver lavas. Diagrams of rare earth element ratios (La/Yb, Gd/Yb, Sm/Yb, La/Sm) indicate that the magmas originate from the partial melting (0.5–5%) of a garnet-lherzolite mantle, suggesting a melting depth greater than 80 km. The low initial $^{87}Sr/^{86}Sr$ ratios: 0.7016–0.7043 and positive εNd isotope of the basaltic lavas confirm their mantle origin. The isotopic data from the Ziver lavas ($^{143}Nd/^{144}Nd$ versus $^{87}Sr/^{86}Sr$) position the samples on the mantel array, with no significant influence on the continental crust. In addition, the Nb/Y versus Zr/Y diagram places the compositions within the field of mantle feather-type sources (OIB), notably HIMU-EM1, confirming an origin linked to intraplate activity or a mantle thermal anomaly. The relationships between the ratios of the different trace elements (Nb/Y and Rb/Y) demonstrate a magmatic differentiation process mainly controlled by fractional crystallization with a negligible contribution from crustal assimilation, as confirmed by the strong chemical distinction from the Precambrian basement around Ziver.

Acknowledgements

This article is part of a Doctoral thesis in progress by the first author. The current work was financially supported by the CNRS–IRD–LithoCOAC project. The authors would like to thank Fabienne De Parseval for thin sections preparation, Philippe De Parseval, Sophie Gouy, and Sophie Mandrou for their technical assistance, respectively during electron microprobe and TIMS analyses. We also thank two anonymous reviewers for their significant and constructive comments, and the editorial assistance of Adenise Lopes.

Declaration of interests

The authors do not work for, advise, own shares in, or receive funds from any organization that could benefit from this article, and have declared no affiliations other than their research organizations.

References

Adams, A. N., D. A. Wiens, A. A. Nyblade, G. G. Euler, P. J. Shore and R. Tibi, "Lithospheric instability and the source of the Cameroon Volcanic Line: evidence from Rayleigh wave phase velocity tomography", *J. Geophys. Res.* **120** (2015), pp. 1708–1727.

Aka, F. T., K. Nagao, M. Kusakabe and N. Nfomou, "Cosmogenic helium and neon in mantle xenoliths from the Cameroon volcanic line (west Africa): preliminary observation", *J. Afr. Earth Sci.* **55** (2009), pp. 175–184.

Asaah, A. N. E., T. Yokoyama, F. T. Aka, et al., "A comparative review of petrogenetic processes beneath the Cameroon Volcanic Line: geochemical constraints", *Geosci. Front.* **6** (2015), pp. 557–570.

Ateba, B., C. Dorbath, L. Dorbath, et al., "Eruptive and earthquake activities related to the 2000 eruption of Mount Cameroon volcano (West Africa)", *J. Volcanol. Geotherm. Res.* **179** (2009), pp. 206–216.

Browne, S. E. and J. D. Fairhead, "Gravity study of the Central African Rift system: a model of continental disruption: the Ngaoundéré and Abu Gabra rifts", *Tectonophysics* **94** (1983), pp. 187–203.

Caldeira, R. and J. M. Munha, "Petrology of ultramafic nodules from São Tomé Island, Cameroon Volcanic Line (oceanic sector)", *J. Afr. Earth.* **34** (2002), pp. 23–246.

Condie, K. C., "High field strength element ratios in Archean basalts: a window to evolving sources of mantle plume", *Lithos* **79** (2005), pp. 491–504.

Corfu, F., S. L. Jackson and R. H. Sutcliffe, "U–Pb ages and tectonic significance of late Archean alkalic magmatism and nonmarine sedimentation: timiskaming group, Southern Abitibi belt, Ontario", *Can. J. Earth Sci.* **28** (1991), pp. 489–503.

Cornacchia, M. and R. Dars, "Un trait structural majeur du continent africain. Les linéaments centrafricains du Cameroun au Golfe d'Aden", *Bull. Soc. Geol. Fr.* **25** (1983), pp. 101–109.

Cox, K. G. and C. J. Hawkesworth, "Geochemical stratigraphy of the Deccan traps at Mahabaleshwar, Western Ghats, India, with implications for open system magmatic processes", *J. Petrol.* **26** (1985), pp. 355–377.

Dasgupta, R., M. M. Hirschmann and N. D. Smith, "Partial melting experiments of peridotite + CO_2 at 3GPa and Genesis of Alkalic Ocean Island Basalts", *J. Petrol.* **48** (2007), pp. 2093–124.

De Plean, R. S. M., I. D. Bastow, E. L. Chambers, D. Keir, R. J. Gallacher and J. Keane, "The development of magmatism along the Cameroon Volcanic Line: evidence from seismicity and seismic anisotropy", *J. Geophys. Res. Solid Earth* **115** (2014), pp. 4233–4252.

Déruelle, B., J.-M. Bardintzeff, J.-L. Cheminée, et al., "Eruptions simultanées de basalte alcalin et de hawaiite au mont Cameroun (28 mars–17 avril 1999)", *C. R. Acad. Sci. Paris, Ser. IIa* **331** (2000), pp. 525–531.

Déruelle, B., C. Moreau, C. Nkoumbou, R. Kambou, J. Lissom, E. Njonfang, R. T. Ghogomu and A. Nono, "The Cameroon Line: a review", in *Magmatism in Extensional Structural Settings* (Kampunzu, A. B. and R. T. Lubala, eds.), Springer: Berlin, 1991, pp. 274–327.

Déruelle, B., J. N'ni and R. Kambou, "Mount Cameroon: an active volcano of the Cameroon line", *J. Afr. Earth Sci.* **6** (1987), pp. 197–214.

Déruelle, B., I. Ngounouno and D. Demaiffe, "The "Cameroon Hot Line (CHL)": a unique example of active alkaline intraplate structure in both oceanic and continental lithospheres", *C. R. Géosci.* **339** (2007), pp. 589–600.

Dick, H. J. B., "Abysal peridotites, very slow spreading ridges and ocean ridge magmatism", in *Magmatism in the Ocean Basins* (Sauders, A. D. and M. J. Norry, eds.), Geological Society, London, Special Publications 42, Geological Society of London, 1989, pp. 71–105.

Dili-Rake, J., S. A. Abdoulaye, J. L. Tchop, M. I. Teitchou, C. Mana Bouba, O. F. Nkouandou, D. Daouda and E. F. Mbossi, "Magmatism of the Beka volcanic massifs (Cameroon Volcanic Line, West-Central Africa): new petrographical and mineralogical data", *J. Geosci. Environ. Prot.* **10** (2022), pp. 198–228.

Djamilatou, D. H., M. Gountié Dedzo, N. Lenhardt, D. Tsozué, N. E. Asaah Asobo and N. M. Klamadji, "Crystallisation and petrogenesis of Cenozoic alkaline basaltic lavas on the Kapsiki Plateau (Moukoulvi, Far-North Cameroon): unveiling the mantle's heterogeneity and HIMU signature", *Solid Earth Sci.* **10** (2025), no. 2, article no. 100231.

Djerossem, F. N., B. J. Mbassa, O. Vanderhaeghe and M. Grégoire, "The Iriba alkaline basalts, an expression of mantle-derived Cretaceous magmatism of the Cameroon–Chad volcanic line along the Central Africa rift system", *C. R. Géosci.* **356** (2024), pp. 231–248.

Dorbath, L., C. Dorbath, G. W. Stuart and J. D. Fairhead, "Structure de la croûte sous le plateau de l'Adamaoua (Cameroun)", *C. R. Acad. Sci. Paris* **298** (1984), pp. 539–542.

Ebinger, C. J. and N. H. Sleep, "Cenozoic magmatism throughout east Africa resulting from impact of a single plume", *Nature* **395** (1998), pp. 788–791.

Fagny, A. M., O. F. Nkouandou, J.-M. Bardintzeff, H. Guillou, G. O. Iancu, N. Z. N. Njankouo and R. Temdjim, "Petrology and geochemistry of the Tchabal Mbabo volcano in Cameroon volcanic line (Cameroon, Central Africa): an intracontinental alkaline volcanism", *J. Afr. Earth Sci.* **170** (2020), article no. 103832.

Fishwick, S., "Surface wave tomography: imaging of the lithosphere–asthenosphere boundary beneath central and southern Africa", *Lithos* **120** (2010), pp. 633–673.

Fitton, J. G., "The Cameroon Line, West Africa: a comparison between oceanic and continental volcanism", in *Alkaline Igneous Rocks* (Fitton, J. G. and B. G. J. Upton, eds.), Geological Society, London, Special Publication, 30, 1987, pp. 273–291.

Fitton, J. G. and H. M. Dunlop, "The Cameroon line, West Africa and its bearing on the origin of oceanic and continental alkali basalt", *Earth Planet. Sci. Lett.* **72** (1985), pp. 23–38.

Fitton, J. G., A. D. Saunders, M. J. Norry, B. S. Hardarson and R. N. Taylor, "Thermal and chemical structure of the Iceland plume", *Earth Planet. Sci. Lett.* **153** (1997), pp. 197–208.

Fosso, J., J. J. Ménard, J.-M. Bardintzeff, P. Wandji, F. M. Tchoua and H. Bellon, "Les laves du mont Bangou: une première manifestation volcanique éocène, à affinité transitionnelle, de la Ligne du Cameroun", *C. R. Géosci.* **337** (2005), pp. 315–325.

Foucarde, S., "Les isotopes: effets isotopiques, bases de radiogéochimie", in *Introduction à la géochimie et ses applications* (Hagemann, G. and M. Treuil, eds.), CEA: Paris, 1998, pp. 265–495.

Gallacher, R. and I. Bastow, "The development of magmatism along the Cameroon Volcanic Line: evidence from teleseismic receiver functions", *Tectonics* **31** (2012), article no. TC3018.

Gass, G., D. Chapman, N. Pollack and R. Thorpe, "Geological and geophysical parameters of mid-plate volcanism", *Philos. Trans. R. Soc. Lond. A* **288** (1978), pp. 583–597.

Gountié Dedzo, M., N. E. A. Asobo, E. M. Fozing, et al., "Petrology and geochemistry of lavas from Gawar, Minawao and Zamay volcanoes of the northern segment of the Cameroon Vol-

canic Line (central Africa): constraints on mantle source and geochemical evolution", *J. Afr. Earth. Sci.* **153** (2019), pp. 31–41.

Gountié Dedzo, M., A. Nedelec, A. Nono, T. Njanko, E. Font, P. Kamgang, E. Njonfang and P. Launeau, "Magnetic fabrics of the Miocene ignimbrites from West-Cameroon: implications for pyroclastic flow source and sedimentation", *J. Volcanol. Geotherm. Res.* **203** (2011), pp. 113–132.

Gourgaud, A. and P. M. Vincent, "Petrology of two continental alkaline intraplate series at Emi Koussi volcano, Tibesti, Chad", *J. Volcanol. Geotherm. Res.* **129** (2003), pp. 261–290.

Gurenko, A., K. Hoernle, F. Hauff, H. Schmincke, D. Han, Y. Miura and I. Kaneoka, "Major, trace element and Nd–Sr–Pb–O–He–Ar isotope signatures of shield stage lavas from the central and western Canary Islands: insights into mantle and crustal processes", *Chem. Geol.* **233** (2006), pp. 75–112.

Haggerty, S. E. and L. A. Tompkins, "Subsolidus reactions in Kimberlitic ilmenites: exsolution, reduction and the redox state of the mantle", *Dev. Petrol.* **6** (1984), pp. 335–357.

Halliday, A. N., J. P. Davidson, P. Holden, C. De Wolf, D. C. Lee and J. G. Fitton, "Trace fractionation in plumes and the origin of HIMU mantle beneath the Cameroon line", *Nature* **347** (1990), pp. 523–528.

Halliday, A. N., A. P. Dicken, A. E. Fallick and J. D. Fitton, "Mantle Dynamics: A Nd, Sr, Pb and O isotope study of the Cameroon Line volcanic chain", *J. Petrol.* **29** (1988), pp. 181–211.

Hart, S. R., E. H. Hauri, L. A. Oschmann and J. A. Whitehead, "Mantle plumes and entrainment: isotopic evidence", *Science* **256** (1992), pp. 517–520.

Hofmann, A. W., K. P. Jochum, M. Seufert and W. M. White, "Nb and Pb in oceanic basalts: new constraints on mantle evolution", *Earth Planet Sci. Lett.* **79** (1986), pp. 33–45.

Irvine, T. N. and W. R. A. Barragar, "A guide to the chemical classification of the common volcanic rocks", *Can. J. Earth Sci.* **8** (1971), pp. 523–548.

Itiga, Z., J.-M. Bardintzeff, P. Wotchoko, P. Wandji and H. Bellon, "Tchabal Gangdaba massif in the Cameroon Volcanic Line: a bimodal association", *Arab. J. Geosci.* **7** (2013), no. 11, pp. 4641–4664.

Jagoutz, E., H. Palme, H. Baddenhausen, et al., "The abundances of major, minor, and trace elements in the earth's mantle as derived from primitive ultramafic nodules", in *Proceedings of the 10th Lunar and Planetary Science Conference, Houston*, vol. 2, Pergamon Press: New York, 1979, pp. 2031–2050.

Kagou Dongmo, A., D. Nkouathio, A. Pouclet, J.-M. Bardintzeff, P. Wandji, A. Nono and H. Guillou, "The discovery of late Quaternary basalt on Mount Bambouto: implications for recent widespread volcanic activity in the Southern Cameroon Line", *J. Afr. Earth Sci.* **57** (2010), pp. 96–108.

Kamgang, P., G. Chazot, E. Njonfang, N. B. Tchuimegnie Ngongang and M. F. Tchoua, "Mantle sources and magma evolution beneath the Cameroon Volcanic Line: geochemistry of mafic rocks from the Bamenda Mountains (NW Cameroon)", *Gondwana Res.* **24** (2013), pp. 727–741.

Kamgang, P., E. Njonfang, A. Nono, D. M. Gountie and F. M. Tchoua, "Petrogenesis of a silicic magma system: geochemical evidence from Bamenda Mountains, NW Cameroon, Cameroon Volcanic Line", *J. Afr. Earth Sci.* **58** (2010), pp. 285–304.

King, S. D. and J. Ritsema, "African hot spot volcanism: small-scale convection in the upper mantle beneath cratons", *Science* **290** (2000), pp. 1137–1140.

Koch, F. W., D. Wiens, A. A. Nyblade, P. Shore, R. Tibi, B. Ateba, C. T. Tabod and J. M. Nnange, "Upper mantle anisotropy beneath the Cameroon Volcanic Line and Congo Craton from shear splitting measurements", *Geophys. J. Int.* **190** (2012), pp. 75–86.

Kogarko, L. N., "Alkaline magmatism in the early history of the Earth", *Petrol* **6** (1998), no. 3, pp. 230–236.

Kuepouo, G., J. P. Tchouankoué, T. Nagao and H. Sato, "Transitional tholeiitic basalts in the tertiary Bana volcano-plutonic complex, Cameroon Line", *J. Afr. Earth Sci.* **45** (2006), pp. 318–332.

Labou, I., M. Benoit, L. Baratoux, M. Gregoire, P. Moussa Ndiaye, N. Thebaud, D. Beziat and P. Debat, "Petrological and geochemical study of Birimian ultramafic rocks within the West African Craton: Insights from Mako (Senegal) and Loraboue (Burkina Faso) lherzolite/harzburgite/wehrlite associations", *J. Afr. Earth Sci.* **162** (2020), article no. 103677.

Le Bas, M. J., R. W. Le Maitre, A. Streickeisen and B. Zanettin, "A Chemical classification of volcanic rocks based on the total alkali-silica diagram", *J. Petrol.* **27** (1986), pp. 745–750.

Leeman, W. P. and C. Hawkesworth, "Open magma systems: trace element and isotopic constraints", *J. Geophys. Res.* **91** (1986), pp. 5901–5912.

Lemdjou, Y. B., D. Zhang, J. P. Tchouankoué, J. Hu, N. B. Tchuimegnie Ngongang, L. Soh Tamehe and Y. Yuan, "Elemental and Sr–Nd–Pb isotopic compositions, and K–Ar ages of transitional and alkaline plateau basalts from the eastern edge of the West Cameroon Highlands (Cameroon Volcanic Line)", *Lithos* **358–359** (2020), article no. 105414.

Li, C.-F., X.-H. Li, Q.-L. Li, J.-H. Guoa, X.-H. Li and Y.-H. Yanga, "Rapid and precise determination of Sr and Nd isotopic ratios in geological samples from the same filament loading by thermal ionization mass spectrometry employing a single-step separation scheme", *Anal. Chim. Acta* **727** (2012), pp. 54–60.

Li, C.-F., X.-H. Li, Q.-L. Li, J.-H. Guoa and X.-H. Lia, "Directly determining $^{143}Nd/^{144}Nd$ isotope ratios using thermal ionization mass spectrometry for geological samples without separation of Sm–Nd", *J. Anal. At. Spectrom.* **26** (2011), pp. 2012–2022.

Marzoli, A., E. M. Piccirillo, P. R. Renne, G. Bellieni, M. Lacumin, J. B. Nyobe and A. F. Tongwa, "The Cameroon Volcanic Line revisited petrogenesis of continental basaltic magmas from lithospheric and asthenospheric mantle sources", *J. Petrol.* **41** (2000), pp. 87–109.

Marzoli, A., P. R. Renne, E. M. Piccirillo, F. Castorina, G. Bellieni, A. J. Melfi, J. B. Nyobe and J. N'ni, "Silicic magmas from the continental Cameroon volcanic line (Oku, Bambouto and Ngaoundere): $^{40}Ar/^{39}Ar$ dates, petrology, Sr–Nd–O isotopes and their petrogenetic significance", *Contrib. Mineral. Petrol.* **135** (1999), pp. 133–150.

Mbassa, B. J., E. Njonfang, M. Benoît, et al., "Mineralogy, geochemistry and petrogenesis of the recent magmatic formations from Mbengwi, a continental sector of the Cameroon Volcanic Line (CVL), Central Africa", *Mineral. Petrol.* **106** (2012), pp. 217–242.

Mbowou, G. I. B., C. Lagmet, S. Nomade, I. Ngounouno, B. Déruelle and D. Ohnenstetter, "Petrology of the late cretaceous peralkaline rhyolites (pantellerite and comendite) from Lake Chad, Central Africa", *J. Geosci.* **57** (2012), pp. 127–141.

McDermott, F., F. G. Delfin, M. J. Defant, S. Turner and R. Maury, "The petrogenesis of magmas from Mt. Bulusan and Mayon in the Bicol arc, the Philippines", *Contrib. Mineral. Petrol.* **150** (2005), pp. 652–670.

McDonough, W. F. and S. S. Sun, "The composition of the Earth", *Chem. Geol.* **120** (1995), pp. 223–253.

Mebara, O. F. X., R. Temdjim, M. P. Njombie Wagsong, C. Gilles, F. A. Tiabou, L. Mouafo and E. Njonfang, "Petrography, mineral chemistry and geochemistry of quaternary volcanism from Wakwa plain, Adamawa Massif (Cameroon Volcanic Line, West-central Africa)", *Arab. J. Geosci.* **15** (2022), article no. 1106.

Medza Ekodo, J. M., Y. Mbida, J. Q. Atangana, S. P. Koah and G. E. Ekodeck, "Characteristics of the Mount Cameroon seismicity for the 2005–2015 period (Cameroon, West-Central Africa)", *J. Seismol.* **27** (2023), pp. 95–114.

Moreau, C., J.-M. Regnoult, B. Déruelle and B. Robineau, "A new tectonic model for the Cameroon Line, Central Africa", *Tectonophysics* **139** (1987), pp. 317–334.

Morimoto, N., J. Fabriès, A. K. Ferguson, et al., "Nomenclature of pyroxenes", *Am. Mineral.* **73** (1988), pp. 1123–1133.

Ngako, V., E. Njonfang, F. T. Aka, T. Affaton and J. M. Nnange, "The North–South Paleozoic to quaternary trend of alkaline magmatism from Niger–Nigeria to Cameroon: complex interaction between hotspot and Precambrian faults", *J. Afr. Earth Sci.* **45** (2006), pp. 241–256.

Ngonge, E. D., M. H. B. M. Hollanda, E. Nkonguin Nsifa and F. M. Tchoua, "Petrology of the Guenfalabo ring-complex: an example of a complete series along the Cameroon Volcanic Line (CVL)", *Cameroon. J. Afr. Earth Sci.* **96** (2014), pp. 139–154.

Ngounouno, I. and B. Déruelle, "Données nouvelles sur le volcanisme cénozoïque du plateau Kapsiki (Nord du Cameroun)", *C. R. Acad. Sci. Paris, Ser. IIa* **324** (1997), pp. 285–292.

Ngounouno, I., B. Déruelle and D. Demaiffe, "Petrology of the bimodal cenozoic volcanism of the Kapsiki Plateau (Northernmost Cameroon, Central Africa)", *J. Volcanol. Geotherm. Res.* **102** (2000), pp. 21–44.

Ngounouno, I., B. Déruelle, D. Demaiffe and R. Montigny, "Petrology of the bimodal Cenozoïc volcanism of the Upper Benue valley, northern Cameroon (Central Africa)", *Contrib. Mineral. Petrol.* **145** (2003), pp. 87–106.

Ngounouno, I., B. Déruelle, R. Guiraud and J.-P. Vicat, "Magmatismes tholéiitique et alcalin des demi-grabens crétacés de Mayo Oulo-Léré et de Babouri-Figuil (Nord du Cameroun–Sud du Tchad) en domaine dextension continentale", *C. R. Acad. Sci. Paris, Ser. IIa* **333** (2001), pp. 201–207.

Njome, S. M. and J. M. De Wit, "The Cameroon Line: analysis of an intraplate magmatic province transecting both oceanic and continental lithospheres. Constraints, controversies and models", *Earth Sci. Rev.* **139** (2014), pp. 168–194.

Njonfang, E., P. Kamgang, T. R. Ghogomu and F. M. Tchoua, "The geochemical characteristics of some plutonic-volcanic complexes along the southern part of the Cameroon Line", *J. Afr. Earth Sci.* **14** (1992), pp. 255–266.

Njonfang, E., A. Nono, P. Kamgang, V. Ngako and F. M. Tchoua, "Cameroon Line alkaline magmatism (central Africa): a reappraisal", in *Volcanism and the Evolution of the African Lithosphere* (Beccaluva, L., G. Bianchini and M. Wilson, eds.), Geological Society of America Special Paper, vol. 478, The Geological Society of America, Inc., 2011, pp. 173–197.

Njonfang, E., T. G. Tchuenté, D. Cozzupoli and F. Lucci, "Petrogenesis of the Sabongari alkaline complex, Cameroon line (central Africa): Preliminary petrological and geochemical constraints", *J. Afr. Earth Sci.* **83** (2013), pp. 25–54.

Nkono, C., O. Féménias and D. Demaiffe, "Geodynamic model for the development of the Cameroon Hot Line (Equatorial Africa)", *J. Afr. Earth Sci.* **100** (2014), pp. 626–633.

Nkouandou, O. F., I. Ngounouno and B. Déruelle, "Géochimie des laves basaltiques récentes des zones Nord et Est de Ngaoundéré (Cameroun, Plateau de l'Adamaoua, Afrique centrale): pétrogenèse et nature de la source", *Int. J. Biol. Chem. Sci.* **4** (2010), pp. 984–1003.

Nkoumbou, C., B. Déruelle and D. Velde, "Petrology of Mt Etinde nephelinite series", *J. Petrol.* **36** (1995), pp. 373–395.

Nono, A., B. Déruelle, D. Demaiffe and R. Kambou, "Tchabal Nganha volcano in Adamawa (Cameroon): petrology of a continental alkaline lava series", *J. Volcanol. Geotherm. Res.* **60** (1994), pp. 147–178.

Noudiedie Kamgang, J. A., J. Tcheumenak Kouemo, E. M. Fozing, A. Kagou Dongmo and R. B. Kenfack, "Structural interpretation of lineament from Nlonako area and surroundings: Contribution to Pan-African tectonic reconstruction", *Eur. J. Environ. Earth Sci.* **1** (2020), no. 5, pp. 1–8.

Noutchogwé-Tatchum, C., C. T. Tabod and E. Manguele-Dicoum, "A gravity study of the crust beneath the Adamaoua fault zone, West Africa", *J. Geophys. Eng.* **3** (2006), pp. 82–89.

Pasyanos, M. and A. Nyblade, "A top to bottom lithospheric study of Africa and Arabia", *Tectonophysics* **444** (2007), pp. 27–44.

Pouclet, A., A. Kagou Dongmo, J. M. Bardintzeff, P. Wandji, P. Chakam Tagheu, D. Nkouathio, H. Bellon and G. Ruffet, "The Mount Manengouba, a complex volcano of the Cameroon Line: volcanic history, petrological and geochemical features", *J. Afr. Earth Sci.* **97** (2014), pp. 297–321.

Poudjom Djomani, Y. H., M. Diament and M. Wilson, "Lithospheric structure across the Adamawa plateau (Cameroon) from gravity studies", *Tectonophysics* **273** (1995), pp. 317–327.

Priestley, K., D. McKenzie, E. Debayle and S. Pilidou, "The African upper mantle and its relationship to techtonics and surface geology", *Geophys. J. Int.* **175** (2008), pp. 1108–1126.

Rankenburg, K., J. C. Lassiter and G. Brey, "The role of continental crust and lithospheric mantle in the genesis of Cameroon Volcanic Line lavas: constraints from isotopic variations in lavas and megacrysts from the Biu and Jos Plateaux", *J. Petrol.* **46** (2005), pp. 169–190.

Reusch, A., A. Nyblade, R. Tibi, D. Wiens, P. Shore, A. Bekoa, C. Tabod and J. Nnange, "Mantle transition zone thickness beneath Cameroon: evidence for an upper mantle origin for the Cameroon Volcanic Line", *Geophys. J. Int.* **187** (2011), pp. 1146–1150.

Shellnutt, J. G., T. Y. Lee, P. K. Torng, C. C. Yang and Y. H. Lee, "Late cretaceous intraplate silicic volcanic rocks from the Lake Chad region: an extension of the Cameroon volcanic line?", *Geochem. Geophys. Geosyst.* **17** (2016), pp. 2803–2824.

Smith, J. V. and W. L. Brown, *Feldspar Minerals: Second Revised and Extended Edition*, Springer Verlag: Berlin, Heidelberg, New York, London, Paris, Tokyo, 1988.

Stuart, G. W., J. D. Fairhead, L. Dorbath and C. Borbath, "Aseismic refraction study of the crustalstructure association with the

Adamaoua plateau and Garoua rift, Cameroun, West Africa", *Geophys. J. R. Astron. Soc.* **81** (1985), pp. 1–12.

Suh, C. E., R. S. J. Sparks, J. G. Fitton, S. N. Ayonghe, C. Annen, R. Nana and A. Luckman, "The 1999 and 2000 eruption of mount Cameroon: eruption behaviour and petrochemistry of lava", *Bull. Volcanol.* **65** (2003), pp. 267–281.

Sun, S. S. and W. F. McDonough, "Chemical and isotopic systematics of oceanic basalts: implications for mantle composition and processes", in *Magmatism in the Ocean Basins* (Saunders, A. D. and M. J. Norry, eds.), Geological Society, London, Special Publications 42, Geological Society of London, 1989, pp. 313–345.

Tamen, J., *Contribution à l'étude géologique du plateau Kapsiki (Extême-Nord Cameroun): volcanologie, pétrologie et géochimie*, Thèse Doct. 3è Cycle, Univ. Ydé I, 1998. 132 p + 53p Annexe + 1 carte. Unpublished.

Tamen, J., C. Nkoumbou, E. Reusser and F. Tchoua, "Petrology and geochemistry of mantle xenoliths from the Kapsiki Plateau (Cameroon Volcanic Line): implications for lithospheric upwelling", *J. Afr. Earth Sci.* **101** (2015), pp. 119–134.

Tchameni, R., F. Sun, D. Dawai, et al., "Zircon dating and mineralogy of the Mokong Pan-African magmatic epidote-bearing granite (North Cameroon)", *Int. J. Earth Sci.* **105** (2016), pp. 1811–1830.

Tchouhla, R., M. G. Dedzo, B. Chako-Tchamabé, et al., "Petrogenesis of lavas from Mokolo-Kosséhone region, northernmost segment of the Cameroon Volcanic Line: constraints from major/trace elements and Sr–Nd–Pb isotopic data", *Geosci. J.* **27** (2023), pp. 139–160.

Tchuimegnie Ngongang, N. B., P. Kamgang, G. Chazot, A. Agranier, H. Bellon and P. Nonnotte, "Age, geochemical characteristics and petrogenesis of Cenozoic intraplate alkaline volcanic rocks in the Bafang region, West Cameroon", *J. Afr. Earth Sci.* **102** (2015), pp. 218–232.

Thierry, P., L. Stieltjes, E. Kouokam, P. Ngueya and P. Salley, "Multihazard risk mapping and assessment on an active volcano: the GRINP project at Mount Cameroon", *Natural Hazards* **45** (2008), no. 3, pp. 429–456.

Vicat, J. P., A. Pouclet, Y. Bellion and J. C. Doumnang, "Les rhyolites hyperalcalines (pantellérites) du lac Tchad. Composition et signification tectonomagmatique", *C. R. Géosci.* **334** (2002), pp. 885–891.

Weaver, B. L., "The origin of ocean island basalt end-member compositions: trace element and isotopic constraints", *Earth Planet. Sci. Lett.* **104** (1991), pp. 381–397.

Weaver, B. L. and J. Tarney, "Empirical approach to estimating the composition of the continental crust", *Nature* **310** (1984), pp. 575–577.

Whitney, D. L. and B. W. Evans, "Abbreviations for names of rock-forming minerals", *Am. Mineral.* **95** (2010), pp. 185–187.

Workman, R. K. and S. R. Hart, "Major and trace element composition of the depleted MORB mantle (DMM)", *Earth Planet. Sci. Lett.* **231** (2005), pp. 53–72.

Yokoyama, T., F. T. Aka, M. Kusakabe and E. Nakamura, "Plume–lithosphere interaction beneath Mt. Cameroon volcano, West Africa: constraints from ^{238}U–^{230}Th–^{226}Ra and Sr–Nd–Pb isotope systematics", *Geochim. Cosmochim. Acta* **71** (2007), pp. 1835–1854.

Youmen, D., H.-U. Schmincke, J. Lissom and J. Etame, "Données géochronologiques: mise en évidence des différentes phases volcaniques au Miocène dans les monts Bambouto (Ligne du Cameroun)", *Sci. Technol. Dev.* **11** (2005), pp. 49–57.

Zellmer, G. F., C. Annen, B. L. A. Charlier, R. M. M. George, S. P. Turner and C. J. Hawkesworth, "Magma evolution and ascent at volcanic arcs: constraining petrogenetic processes through rates and chronologies", *J. Volcanol. Geotherm. Res.* **140** (2005), pp. 171–191.

Ziem à Bidias, L. A., G. Chazot, A. Moundi and P. Nonnotte, "Extreme source heterogeneity and complex contamination patterns along the Cameroon Volcanic Line: new geochemical data from the Bamoun plateau", *C. R. Géosci.* **350** (2018), pp. 100–109.